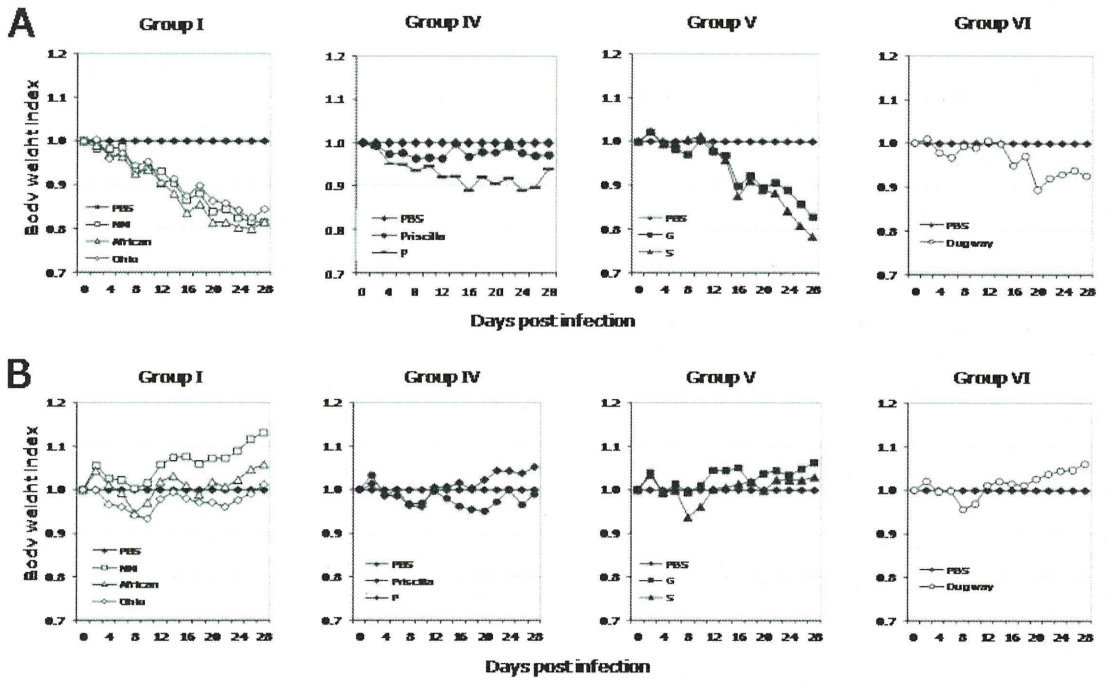

FIG. 1. Average body weight changes in SCID mice (A) and CB-17 mice (B) infected with *C. burnetii* isolates during 28 days of infection. Body weights were significantly lower in SCID mice throughout the infection period and transiently in CB-17 mice infected with all isolates except Priscilla compared to PBS-injected controls ($P < 0.05$).

late resulted in slow, progressive, and long-term-persistent disease. Clinical signs included ruffled fur, extremely distended abdomens, and death. Body weight loss, inactivity, and cachexia were not observed until a few days prior to death. Survival time ranged from 55 to 109 days p.i. Progression of clinical signs and survival times were dose dependent, with shorter times corresponding to higher infectious doses (see Table S2 in the supplemental material). Similar lesions were found in all of the SCID mice that died, most notably severe hepatosplenomegaly, and all organs had cellular infiltration, primarily macrophages containing bacteria. The severity of the lesions in infected SCID mice was not dependent on the *C. burnetii* challenge dose.

On the other hand, CB-17 and A/J mice displayed transitory clinical signs only after infection with the highest dose of Priscilla. Both mouse strains showed ruffled fur from 4 to 13 days p.i., but only A/J mice demonstrated transient body weight loss (data not shown). No other clinical signs were observed. At 28 days p.i., CB-17 and A/J mice had mild splenomegaly and seroconversion as evidence of infection (data not shown). Small granulomas were present in the spleen and liver, but bacterial antigen was not detectable by immunohistochemistry.

Genomic-group-specific virulence in mice. It was important to establish whether the results of infection seen with the Priscilla isolate and those previously noted with the NM isolate were genomic group specific (24). To determine this, the pathogenicities of multiple isolates were compared by delivering a single dose of eight *C. burnetii* isolates from four genomic groups (Table 1) to mice by i.p. injection. The infections were initially compared in SCID and CB-17 mice sacrificed at 28 days p.i.

All *C. burnetii* isolates caused disease in SCID mice, with various clinical courses. There was no mortality during the 28-day infection period. Clinical signs, including significant body weight loss ($P < 0.05$) and cachexia, summarized in Fig. 1A and in Fig. S1A in the supplemental material, were most apparent in mice infected with group I isolates, followed by those given group V, IV, and VI isolates. In CB-17 mice, only mild transient disease was noted, with minimal loss of body weight, in response to all isolates and noticeably ruffled fur with group I isolate infection (Fig. 1B).

Splenomegaly in response to infection was more severe in SCID than in CB-17 mice (Fig. 2A). The number of bacteria in the spleens was determined by qPCR (Fig. 2B), and consistently higher numbers of *com1* genes were detected in SCID than in CB-17 mice. SCID mice showed phylogenetic-group-characteristic spleen size and growth of bacteria. Splenomegaly was greatest in SCID mice with mild clinical disease infected with bacteria from groups IV and VI. However, the number of organisms in the spleen was greater in mice with severe clinical disease following infection with phylogenetic groups I and V. In CB-17 mice, splenic enlargement and numbers of bacteria increased with the severity of clinical disease. CB-17 mice displayed differences between infection with the *C. burnetii* isolates that caused acute disease (phylogenetic group I) and infection with the *C. burnetii* isolates that caused chronic disease (phylogenetic groups IV and V), but there was no difference between groups infected with isolates that caused chronic disease. All infected mice developed significant splenomegaly,

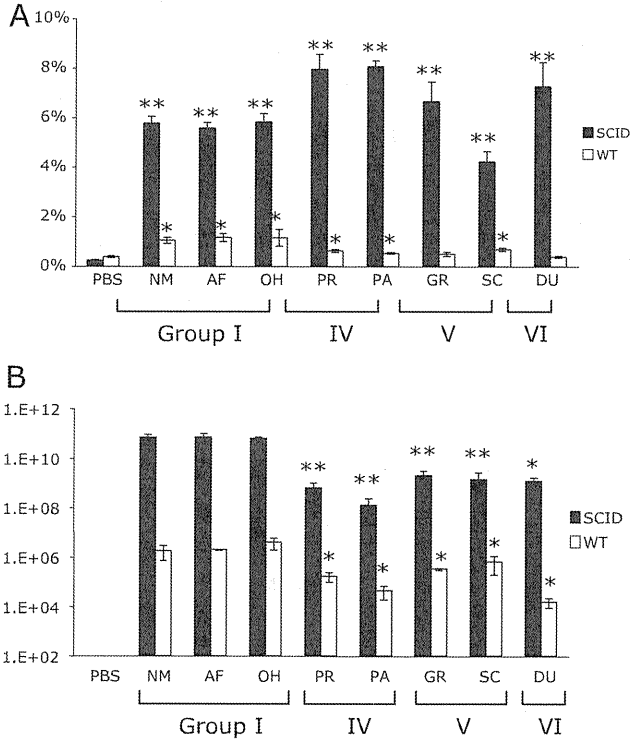

FIG. 2. Splenomegaly (A) and splenic bacterial loads (B) in mice at 28 days p.i. (A) All infected animals developed significant splenomegaly compared to controls, and infected SCID mice had significantly larger spleens than CB-17 mice ($P < 0.05$). (B) Mice infected with group IV, V, and VI isolates had significantly fewer bacteria than those infected with group I isolates ($P < 0.05$). *, $P < 0.05$. The error bars indicate standard deviations.

but mice infected with group IV, V, and VI isolates had significantly fewer splenic bacteria than mice infected with group I isolates ($P < 0.05$).

Evaluation of histopathology at 28 days p.i. revealed more lesions in SCID mice than in CB-17 mice (see Table S3 in the supplemental material). SCID mice showed histopathologic changes in all organs investigated. Group I isolates caused the most inflammation, followed by groups V, IV, and VI. The inflammatory-cell populations were similar in all groups and consisted of few neutrophils and numerous macrophages containing abundant intracytoplasmic bacteria. *C. burnetii* antigen was diffusely distributed in all organs examined. CB-17 mice had mild histopathologic changes in some organs, but even in the tissues with an inflammatory response, *C. burnetii* antigen was rarely detected.

Circulating cytokines are altered in *C. burnetii*-infected CB-17 mice. The variations in pathology and inflammation associated with these isolate group infections suggest differences in the immune responses. To expand on this observation, the serum levels of 16 cytokines and chemokines were measured. In CB-17 mice, serum cytokine levels differed between mice infected with group I isolates and those given isolates from other groups. Group I isolates induced persistently high cytokine secretion throughout the 28-day experiment; group IV and V isolates caused moderate cytokine secretion at the peak of clinical disease (7 to 14 days p.i.) (Fig. 3). After 14 days p.i., group I isolates induced higher secretion of IL-3, IL-4, IL-6, IL-10, IL-12p40, IL-12p70, IFN-γ, TNF-α, MIP-1α, and RANTES than other groups. The KC and granulocyte-macrophage colony-stimulating factor levels of mice infected with group I isolates were higher than those in mice infected with other groups prior to 14 days p.i. Serum IL-1α, IL-1β, IL-2, and IL-5 levels and eotaxin secretion were not increased during the infection period (data not shown).

Lethal potentials of all genomic groups in SCID mice. The lethal potentials of representative isolates from each phylogenetic group were investigated in SCID mice, and it was determined that all of the isolates evaluated could eventually lead to clinical illness and death in the immunodeficient model (see Fig. S1B in the supplemental material). Isolates that caused a long period of cachexia led to severe body weight loss in infected mice (see Fig. S2 in the supplemental material). A group I isolate (NM) induced the earliest and longest period of cachexia and, correspondingly, the most severe body weight loss. Mice infected with isolates from groups V (G) and VI (Dugway) had similar survival times, but those given group V isolates had longer periods of cachexia and more severe body weight loss than group VI-infected mice. Infection with group IV isolates (Priscilla and P) resulted in the shortest period of cachexia, and body weight loss was not observed until the terminal stage of infection. The survival time was shortest in mice challenged with group I isolates (32.0 ± 0.8 days), followed by those infected with groups V (36.0 ± 0.0 days), VI (35.5 ± 1.0 days), and IV (47.5 ± 0.6 days for P and 77.3 ± 2.8 days for Priscilla). The probable cause of death was multiple-organ failure due to massive systemic infection.

The pathological changes in SCID mice at mortality were more advanced than those observed at 28 days p.i. (data not shown). The severity of inflammatory changes in the liver and spleen was similar in all groups of infected mice, but animals given group I isolates exhibited a greater degree of inflammation in the heart and lungs than those given group IV, V, and VI isolates. The extent of splenomegaly changed with survival time; however, the numbers of bacteria in the spleen were similar in all groups, suggesting that the number of bacteria (10^{10} genome copies/spleen) detected is the saturation point in SCID mice. *C. burnetii* antigen was diffusely distributed in all tissue sections.

Genomic-group-specific outcome of acute Q fever pneumonia in the guinea pig aerosol model. Aerosol challenge in the guinea pig provides a physiologically relevant model that simulates both the natural route of infection and common clinical presentations associated with human acute Q fever, making this a choice model for evaluating the comparative levels of virulence of different *C. burnetii* isolates, and thus, it was used in the logical progression of experiments after different levels of virulence were observed in mouse models of infection. Guinea pigs challenged with group I and V isolates developed significant fever in response to infection ($P < 0.01$), whereas those given isolates from groups IV and VI were afebrile even at the highest challenge dose (Fig. 4).

Fever response, weight loss, and other clinical signs displayed a dose-dependent relationship in guinea pigs infected with the group I *C. burnetii* isolates African and Ohio, as has been described for the reference isolate in this group, NM (43). All animals that received African or Ohio organisms at a high

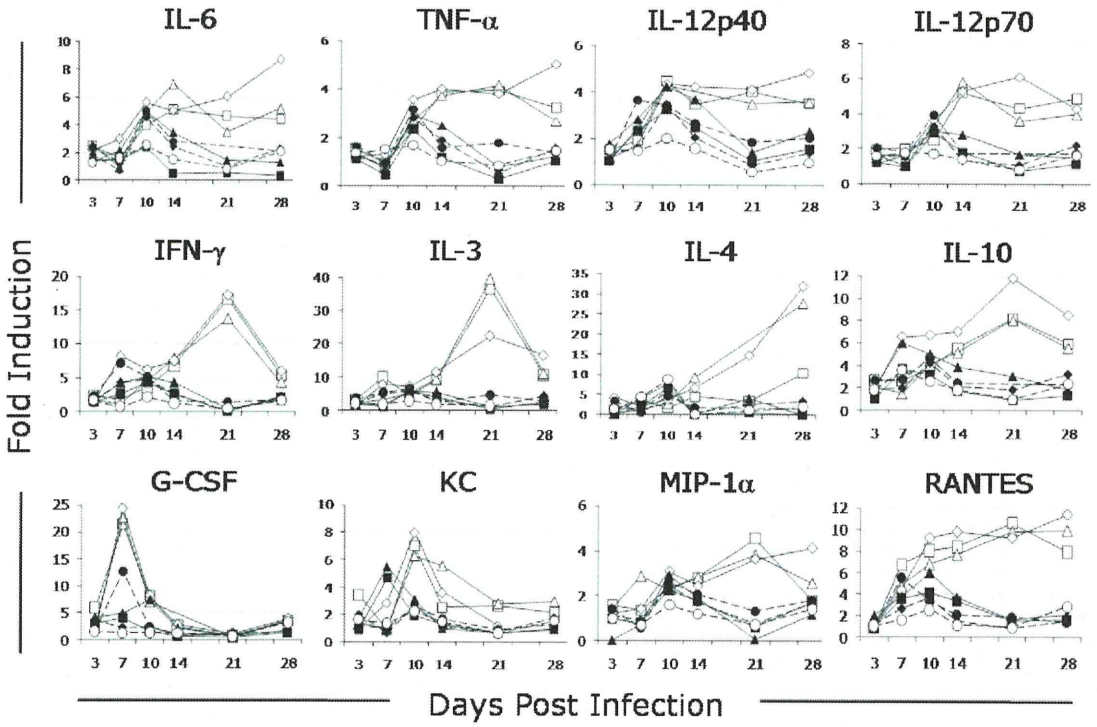

FIG. 3. Mean circulating cytokine levels in response to infection in CB-17 mice with different *C. burnetii* isolates. Isolates from genomic group I induced persistently high cytokine secretion with increased levels of IL-6, TNF-α, IL-12p40, IL-12p70, IFN-γ, IL-3, IL-4, IL-10, MIP-1α, and RANTES compared with other genogroups ($P < 0.05$). ◆, PBS; □, NM; △, African; ◇, Ohio; ●, Priscilla; ◆, P; ■, G; ▲, S; ○, Dugway.

dose died within 7 to 9 days p.i., as did two of three that received NM; lower infectious doses were not lethal. Gross lung consolidation and overall lack of normal body fat were noted on necropsy at 7 to 9 days p.i. in guinea pigs infected with the highest dose of organisms. Histologically, these animals had severe panleukocytic bronchointerstitial pneumonia with bronchial and alveolar exudates. Lung tissues from the surviving NM-infected guinea pig and those given the mid-level dose of group I organisms were evaluated at 28 days p.i. for comparison to animals infected with other isolates evaluated at this time, and they exhibited moderate multifocal lymphohistiocytic pneumonia with granuloma formation.

No significant fever or other overt clinical signs were noted in guinea pigs infected with group IV isolates. Mild lymphohistiocytic pneumonia was seen histologically at 28 days p.i. in animals given the highest dose of organisms.

Group V isolate-infected guinea pigs all developed fever when given the highest challenge dose, and dose-dependent temperature increases and other clinical signs were again noted, with no fever development, in those animals receiving the lowest dose of organism. Though auscultation confirmed respiratory compromise, none of the infections were lethal. At 28 days p.i., the lungs had mild to moderate lymphohistiocytic interstitial pneumonia and a few small granulomas.

No major clinical or pathological changes were noted in guinea pigs infected with the group VI isolate or in negative control animals. Table S4 in the supplemental material compares the severity of histopathologic changes in guinea pigs infected with high doses of *C. burnetii* isolates from each group at 28 days p.i. Immunohistochemistry confirmed the presence of *C. burnetii* organisms, primarily in macrophages, in the lungs, livers, and spleens of infected animals.

Experimental guinea pigs in all dose groups for each isolate seroconverted by the time of euthanasia, with the exception of animals infected with high doses of NM, African, and Ohio necropsied at 1 week p.i. and low-dose Dugway-infected guinea pigs. The degree of seroconversion was dose dependent and varied among isolates (data not shown). No PBS-injected control animals seroconverted.

Genomic-group-specific severity of hepatitis and splenomegaly in guinea pigs. The doughnut granulomas common in human acute Q fever hepatitis (31) had not been previously described in animals experimentally infected with *C. burnetii* and were also not seen in the guinea pigs in this study. Mild hepatitis and severe hepatic lipidosis were noted at death 7 days p.i. in guinea pigs challenged with high doses of group I isolates, as had been previously reported for NM aerosol-infected guinea pigs (43). Tissue sections from the remaining NM-infected guinea pig and those infected with mid-level doses of the group I organisms were evaluated for comparison with animals infected with other isolates at 28 days p.i. and revealed vacuolization and degeneration of centrilobular hepatocytes, lymphocyte infiltration in periportal regions, and multiple small granulomas.

Group IV-infected guinea pigs also had periportal lymphocytic infiltration, as well as multiple granulomas of various sizes. The granulomas in Priscilla- and P-infected guinea pigs were more defined, with more histiocytic involvement than was

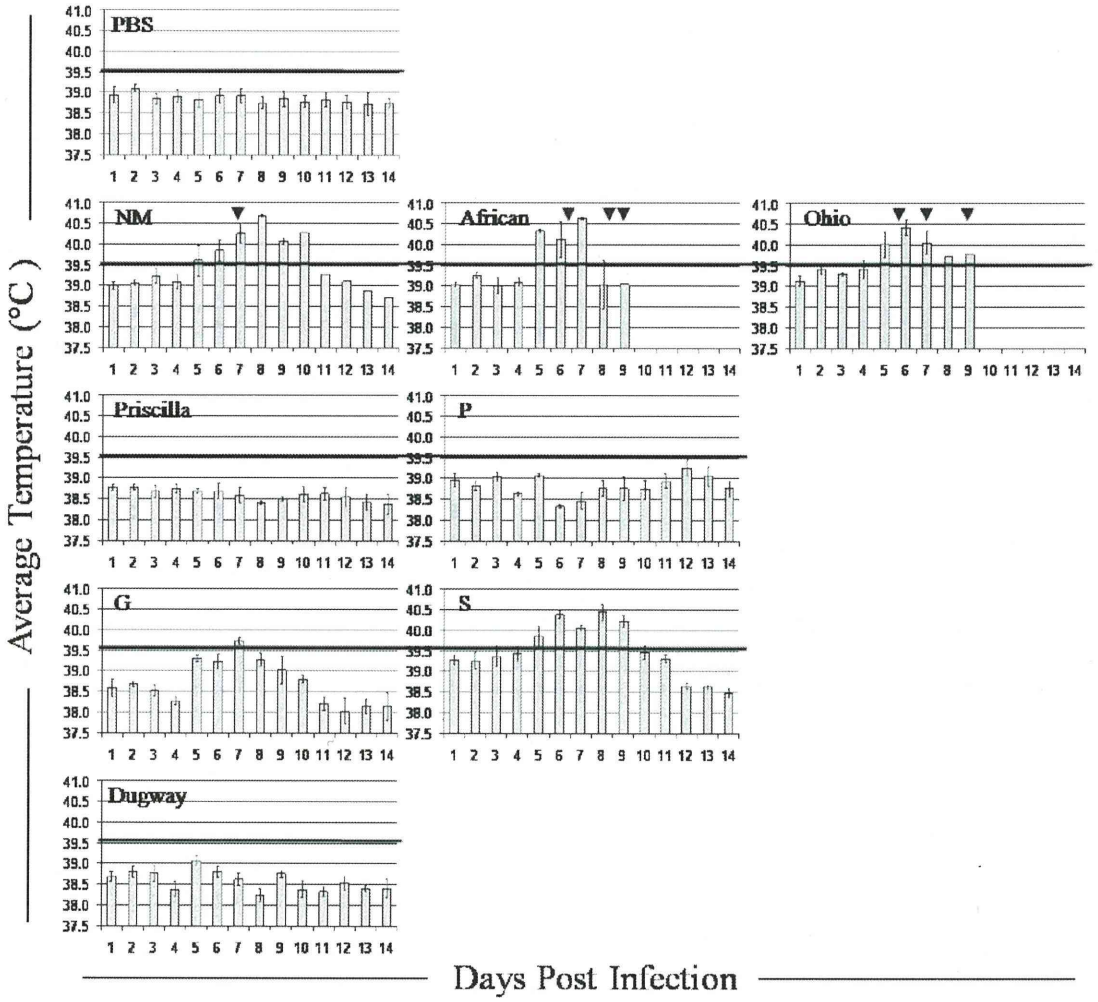

FIG. 4. Fever responses of guinea pigs to infection with high doses of *C. burnetii* isolates. The mean daily temperatures ± standard errors of the mean ($n = 3$) of animals infected with 2×10^6 bacteria of each *C. burnetii* isolate. Temperatures of ≥39.5°C (black lines) were considered fever. The arrows indicate days on which death occurred in NM-, African-, and Ohio-infected groups.

seen in guinea pigs infected with group I isolates. Subjectively, of all animals necropsied from each isolate group, hepatic granulomas from those infected with P were the greatest in size and number.

The livers of guinea pigs infected with the group V isolates G and S contained a few small granulomas and mild to moderate infiltration of lymphocytes along portal tracts. The hepatic changes observed in guinea pigs infected with group V isolates suggested that isolates from this group are less hepatovirulent than group IV isolates but more so than group I isolates.

No hepatic granulomas or other significant pathological changes were noted in guinea pigs infected with the group VI isolate Dugway. Liver weights did not vary significantly within or between genomic groups.

There were no significant differences in spleen weights at 28 days p.i. within or between genomic or dose groups. Animals infected with all isolates examined at 14 days p.i. (NM, P, G, and Dugway) had significantly larger spleens than PBS-injected control animals, and spleens from NM- and G-infected guinea pigs were significantly larger ($P < 0.01$ and $P < 0.05$, respectively) than those of P- and Dugway-infected animals (see Fig. S3 in the supplemental material). Pathological findings included multiple small granulomas in the spleens of group I-infected guinea pigs; fewer small granulomas were occasionally noted in animals infected with group IV and V isolates.

Heterologous protection of cross-vaccination and challenge in guinea pigs. The infection studies described here illustrate that there is pathotype diversity between *C. burnetii* isolates from different genogroups, and they are consistent with phylogenetic studies cataloging distinct gene contents (4). We therefore strove to determine whether this diversity was great enough to affect the ability of vaccines to protect against infection. Guinea pigs were given group I (NM) or group IV (S) vaccine and cross-challenged to evaluate potential heterologous protection against high-dose infection. Nonvaccinated guinea pigs developed a noticeable fever response by day 5 p.i.,

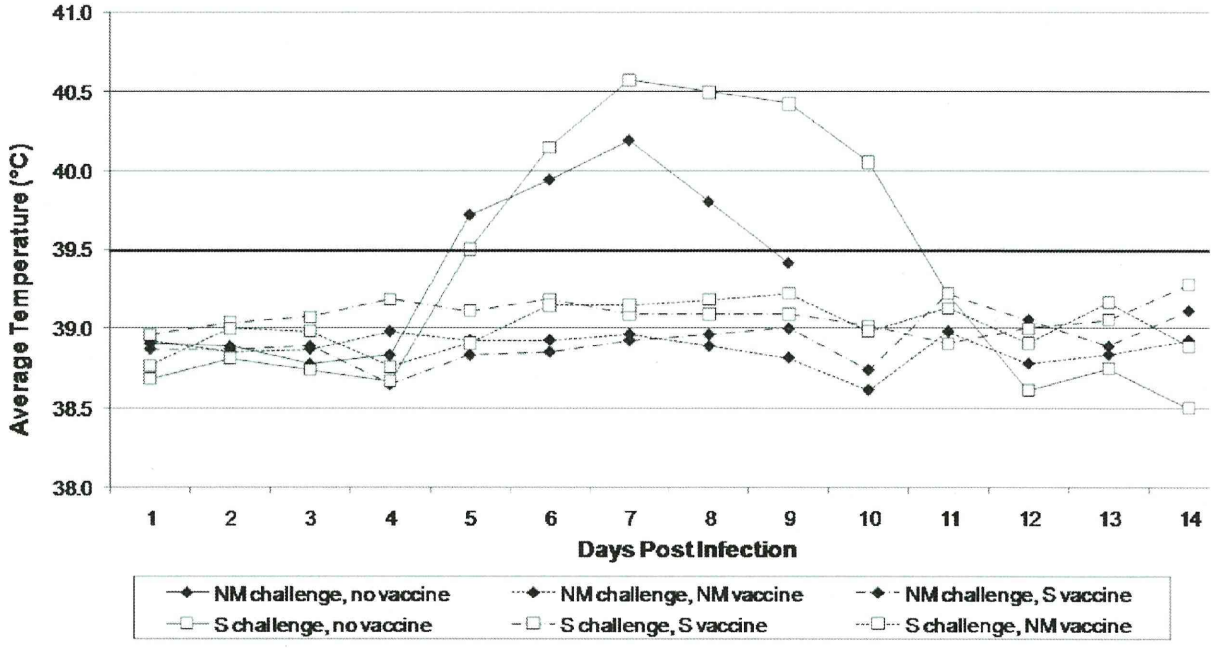

FIG. 5. Heterologous vaccination and challenge in guinea pigs. Shown are average daily temperatures of animals vaccinated with NM (dashed and dotted line), S (dashed line), or adjuvant alone (solid line) and challenged with high doses of NM (◆) or S (□). Temperatures of ≥39.5°C were considered fever.

and infection was lethal in three of three NM- and one of three S-challenged animals. Guinea pigs vaccinated with either formalin-killed NM or S were completely protected against fever development and death when challenged with either NM or S (Fig. 5).

DISCUSSION

The potential for genomic-group-specific pathogenicity of *C. burnetii* was evaluated using immunocompetent mice and guinea pigs and immunodeficient mice. The hypotheses that isolates belonging to the same genomic group would cause similar disease and that there would be distinctions in disease manifestations between isolate groups were supported by the findings presented here.

A detailed analysis of the Priscilla isolate dose-effect in SCID mice revealed differences in virulence of *C. burnetii* isolates. Disease development after Priscilla infection was progressive but slower than the development of the disease caused by NM previously reported in SCID mice (1); the survival time of SCID mice infected with Priscilla was longer with the same LD_{50}. This result supports the previous study by Moos and Hackstadt that evaluated the lesser ability of the Priscilla isolate to cause fever in i.p.-challenged guinea pigs (36). Interestingly, the mice infected with Priscilla did not exhibit cachexia until the terminal stages of infection, when they had extremely severe hepatosplenomegaly. Although the disease caused by Priscilla was milder than that associated with NM, all mice that developed clinical illness died. This result confirms the high infectivity and lethal potential of *C. burnetii*, which is not restricted to isolates that cause acute disease, and suggests that the SCID mouse model can be useful for evaluation of *C. burnetii* virulence.

The virulence of *C. burnetii* isolates tested in SCID mice was determined to be genomic group specific. Acute-Q fever-associated group I isolates caused the most rapidly progressing disease and the most severe pathological changes. Groups IV and V, isolates associated with chronic Q fever, caused a slower progression of disease. Overall, pathological changes in mice infected with group IV and V isolates were milder than those of group I-infected mice. The number of bacteria in the spleen at 28 days p.i. was greater in mice with severe disease from infection with group I isolates; however, the bacterial loads at the time of death were similar in all infected mice. This suggests that the rate of proliferation of *C. burnetii* in vivo may be virulence related. An in vitro comparison of infection in L929 cells using NM, Priscilla, and S isolates showed that all of the isolates could persistently infect, but Priscilla required a greater period of time to establish an infection (42), and it has been shown that inclusion-forming units produced by NM and Priscilla isolates were similar in Vero cells (36). However, because of developmental differences in clinical signs and pathological changes, the replication rate does not seem to be the only virulence factor involved, since clinical signs would then be similar with differences only in disease progression. At both time points, 28 days p.i. and the time of death due to infection, heart and lung lesions caused by group IV, V, and VI isolates were milder than those produced by infection with group I isolates. This observation seems to conflict with the hypothesis that isolates from chronic disease cause chronic Q fever, including heart disease. However, our observation is consistent with the report that isolates from heart lesions of

chronic-Q fever patients have genetic characteristics similar to those of isolates from acute disease (46). The hypothesis that isolates from acute disease do not cause endocarditis has been supported by two other research groups (17, 24). The correlation between virulence and phylogeny has been controversial because of a lack of comprehensive studies. One study detected genes specific to isolates from acute disease in isolates from chronic Q fever patients and concluded that the isolates were not disease specific (46). The isolates used in the study were isolated by cell culture, and although the cell culture system is highly effective for isolation, isolates from acute disease are known to infect cultured cells more efficiently than isolates from chronic disease, so there remains a potential that the study collected only cell culture-adapted isolates. Several in vivo studies have reported isolate-specific virulence using guinea pig and mouse models (17, 24, 36); however, the number of isolates used in these studies was limited, making it difficult to conclude that there was genomic-group-specific virulence. The present study using eight isolates from four phylogenetic groups strongly supports the variation in virulence among *C. burnetii* isolate groups.

In the absence of functional T and B cells, cytokine profiles showed no group-specific differences. In immunocompetent mice, group I isolates caused a stronger immune response with high levels of multiple cytokines over a longer time than other groups. Interestingly, Dugway (group VI) induced the least change in CB-17 mice. The inflammatory-cytokine changes in immunocompetent mice in this study were similar to those in humans with acute Q fever (10): TNF-α and IL-6 were upregulated, but IL-1β was not. IFN-γ increased in CB-17 mice infected with group I isolates, and it is associated with the control of bacterial growth, stimulates phagosome-lysosome fusion, and may enable monocytes/macrophages to kill *C. burnetii* (13, 14). A difference in vacuole formation between isolates has also been shown, with NM and S developing within single large vacuoles while Priscilla occupied several smaller vacuoles per cell (18). This in vitro study suggested a difference in isolate ecology within host cells, which may be correlated with their virulence in vivo.

The ability to cause fever and respiratory illness was isolate and dose dependent in the guinea pig aerosol challenge model, with isolates from groups I and V causing disease consistent with human acute Q fever. Isolates within the same genomic group produced similar clinical illnesses, strongly supporting the mouse experiments demonstrating that genomic differences in the bacterial isolates do play a role in virulence. It was shown here that isolates associated with chronic disease, G and S, have the ability to cause acute disease in the guinea pig model. Our study confirmed and expanded the observations of Kazar et al. that the virulence of NM and S isolates was greater than that of Priscilla.

Lesny et al. compared the cross-immunity of whole-cell and soluble Q fever vaccines made from phase I NM, S, Priscilla, and Luga isolates. They found that vaccines from NM and Priscilla afforded a higher degree of protection than S and Luga vaccines and that whole-cell vaccines were more effective than soluble vaccines (28). In the guinea pig challenge study presented here, killed whole-cell vaccines made from isolates differing in LPS banding pattern (16), plasmid type (44), and genomic group (20), specifically isolates from groups I and V, conferred heterologous protection against virulent high-dose challenge in accordance with previous studies (28). This suggests that although the manifestations of disease and genomic contents differ among various isolate groups, the antigenic properties of whole-cell vaccines are shared enough that cross-protection is possible. Such information is valuable for the design of new vaccines and could be of the utmost importance in offering reliable protection in the event of an outbreak.

The differences in perceived infectious doses noted when ODs, particle counts, and genome copy enumerations were compared underline the importance of using multiple quantitation methods to compare studies with earlier observations. Some of the differences in disease manifestations seen in guinea pigs in this study could be due to slight differences in the infectious doses delivered. For instance, Priscilla and P both induced hepatic changes, although guinea pigs infected with P appeared to develop more severe lesions than those infected with Priscilla, which had a lower infectious dose by OD and qPCR. The difference in infectious dose as determined by the genome copy number could account for this variation. However, G and S both caused fever, and although guinea pigs infected with G did not attain the same degree of febrile response as S-infected animals, quantitation by particle count and real-time PCR showed infectious doses of S to be over a log unit lower than those of G. It could be argued that Priscilla-infected guinea pigs did not develop fever because fewer bacteria were present in the aerosol challenge; however, the group IV isolates did not induce fever at any of the challenge doses while group I isolates induced fever even at the lowest dose. We believe that, despite the variation in the infectious dose depending on the enumeration technique, the significant differences noted among genotypic groups are valid.

Phase variation is the only well-characterized phenotypic difference that is related to virulence in *C. burnetii* (50). Although LPS may be a major virulence determinant, and isolate LPS banding patterns have been correlated with acute or chronic disease (16), other components alone or in association with LPS may be responsible for differences in mortality in SCID mice and fever development in aerosol-challenged guinea pigs. It has been hypothesized that differences in the lipid A component are responsible for the variations in virulence, but lipid structural information indicates they are similar. The combination of a variety of factors expressed by phase I bacteria likely governs the ability of *C. burnetii* to infect cells and to maintain continuous growth within the phagolysosome. Indeed, the combination of pathotype variation of disease in infected guinea pigs and cross-protection of different isolates suggests conserved predominant antigenic components with virulence determinant specificity.

A recent report compared all open reading frames of NM phase I to those of African, Ohio, P, G, S, and Dugway, among others (4), and a majority of the open reading frames deleted from NM in the other isolates were either hypothetical or nonfunctional; however, a few were associated with assorted cellular functions. Beare et al. compared the complete genome sequences of NM, K, G, and Dugway and found distinct collections of pseudogenes and unique gene contents that may contribute to pathotype-specific virulence, including type II and type IV secreted effector molecules (5). Integrating our in vivo data with these molecular details, as well as with other in

vitro studies, may reveal the critical virulence determinants of *C. burnetii* and ultimately identify targets for vaccine and therapeutic intervention.

Isolates of phase I *C. burnetii* have the potential to cause a range of clinical signs, including fever, pneumonia, hepatitis, and splenomegaly. Isolates from one human chronic-disease group induced mild to moderate acute disease in the physiologically relevant guinea pig aerosol challenge model, while a separate isolate group representing several chronic-disease isolates caused no acute disease. All isolates examined were capable of producing disease in the immunocompromised SCID mouse model, and genogroup-consistent trends were noted in cytokine production in response to infection in the immunocompetent-mouse model. In these studies, isolates within the same genomic group caused similar pathological responses, with a distinction in strain virulence between established genogroups, sustaining the theory that genetic differences in the bacterial isolates affect their virulence.

ACKNOWLEDGMENTS

This work was supported by funding from NIH NIAID grants KO8 AI055664, U54 AI057156, and RO1 AI057768 and Science Research Grant number 13460142 from the Ministry of Education, Science, Sports and Culture of Japan.

We are grateful to Laura R. Hendrix for critical review of the manuscript.

REFERENCES

1. **Andoh, M., T. Naganawa, A. Hotta, T. Yamaguchi, H. Fukushi, T. Masegi, and K. Hirai.** 2003. SCID mouse model for lethal Q fever. Infect. Immun. **71:**4717–4723.
2. **Arricau-Bouvery, N., Y. Hauck, A. Bejaoui, D. Frangoulidis, C. C. Bodier, A. Souriau, H. Meyer, H. Neubauer, A. Rodolakis, and G. Vergnaud.** 2006. Molecular characterization of *Coxiella burnetii* isolates by infrequent restriction site-PCR and MLVA typing. BMC Microbiol. **6:**38.
3. **Baumgartner, W., H. Dettinger, N. Schmeer, and E. Hoffmeister.** 1988. Evaluation of different fixatives and treatments for immunohistochemical demonstration of *Coxiella burnetti* in paraffin-embedded tissues. J. Clin. Microbiol. **26:**2044–2047.
4. **Beare, P. A., J. E. Samuel, D. Howe, K. Virtaneva, S. F. Porcella, and R. A. Heinzen.** 2006. Genetic diversity of the Q fever agent, *Coxiella burnetii*, assessed by microarray-based whole-genome comparisons. J. Bacteriol. **188:**2309–2324.
5. **Beare, P. A., N. Unsworth, M. Andoh, D. E. Voth, A. Omsland, S. D. Gilk, K. P. Williams, B. W. Sobral, J. J. Kupko III, S. F. Porcella, J. E. Samuel, and R. A. Heinzen.** 2008. Comparative genomics reveal extensive transposon-mediated genomic plasticity and diversity among potential effector proteins within the genus *Coxiella*. Infect. Immun. **77:**642–656.
6. **Benenson, A. S., and W. D. Tigertt.** 1956. Studies on Q fever in man. Trans. Assoc. Am. Physicians **69:**98–104.
7. **Benoit, M., E. Ghigo, C. Capo, D. Raoult, and J. L. Mege.** 2008. The uptake of apoptotic cells drives *Coxiella burnetii* replication and macrophage polarization: a model for Q fever endocarditis. PLoS Pathog. **4:**e1000066.
8. **Brennan, R. E., and J. E. Samuel.** 2003. Evaluation of *Coxiella burnetii* antibiotic susceptibilities by real-time PCR assay. J. Clin. Microbiol. **41:**1869–1874.
9. **Brouqui, P.** 1993. Chronic Q fever. Arch. Inern. Med. **153:**642–648.
10. **Capo, C., N. Amirayan, E. Ghigo, D. Raoult, and J. Mege.** 1999. Circulating cytokine balance and activation markers of leucocytes in Q fever. Clin. Exp. Immunol. **115:**120–123.
11. **Capo, C., Y. Zaffran, F. Zugan, P. Houpikian, D. Raoult, and J. L. Mege.** 1996. Production of interleukin-10 and transforming growth factor β by peripheral blood mononuclear cells in Q fever endocarditis. Infect. Immun. **64:**4143–4150.
12. **Ghigo, E., C. Capo, D. Raoult, and J. L. Mege.** 2001. Interleukin-10 stimulates *Coxiella burnetii* replication in human monocytes through tumor necrosis factor down-modulation: role in microbicidal defect of Q fever. Infect. Immun. **69:**2345–2352.
13. **Ghigo, E., C. Capo, C. H. Tung, D. Raoult, J. P. Gorvel, and J. L. Mege.** 2002. *Coxiella burnetii* survival in THP-1 monocytes involves the impairment of phagosome maturation: IFN-gamma mediates its restoration and bacterial killing. J. Immunol. **169:**4488–4495.
14. **Ghigo, E., A. Honstettre, C. Capo, J. P. Gorvel, D. Raoult, and J. L. Mege.** 2004. Link between impaired maturation of phagosomes and defective *Coxiella burnetii* killing in patients with chronic Q fever. J. Infect. Dis. **190:**1767–1772.
15. **Glazunova, O., V. Roux, O. Freylikman, Z. Sekeyova, G. Fournous, J. Tyczka, N. Tokarevich, E. Kovacava, T. J. Marrie, and D. Raoult.** 2005. *Coxiella burnetii* genotyping. Emerg. Infect. Dis. **11:**1211–1217.
16. **Hackstadt, T.** 1986. Antigenic variation in the phase I lipopolysaccaride of *Coxiella burnetii* isolates. Infect. Immun. **52:**337–340.
17. **Hackstadt, T.** 1990. The role of lipopolysaccharides in the virulence of *Coxiella burnetii*. Ann. N. Y. Acad. Sci. **590:**27–32.
18. **Hechemy, K. E., M. McKee, M. Marko, W. A. Samsonoff, M. Roman, and O. Baca.** 1993. Three-dimensional reconstruction of *Coxiella burnetii*-infected L929 cells by high-voltage electron microscopy. Infect. Immun. **61:**4485–4488.
19. **Hendrix, L., and L. P. Mallavia.** 1984. Active transport of proline by *Coxiella burnetii*. J. Gen. Microbiol. **130:**2857–2863.
20. **Hendrix, L. R., J. E. Samuel, and L. P. Mallavia.** 1991. Differentiation of *Coxiella burnetii* isolates by analysis of restriction-endonuclease-digested DNA separated by SDS-PAGE. J. Gen. Microbiol. **137:**269–276.
21. **Honstettre, A., G. Imbert, E. Ghigo, F. Gouriet, C. Capo, D. Raoult, and J. L. Mege.** 2003. Dysregulation of cytokines in acute Q fever: role of interleukin-10 and tumor necrosis factor in chronic evolution of Q fever. J. Infect. Dis. **187:**956–962.
22. **Huebner, R. J., W. L. Jellison, and M. D. Beck.** 1949. Q fever studies in southern California. III. Effects of pasteurization on survival of *Coxiella burnetii* in naturally infected milk. Public Health Rep. **64:**499–511.
23. **Jager, C., H. Willems, D. Thiele, and G. Baljer.** 1998. Molecular characterization of *Coxiella burnetii* isolates. Epidemiol. Infect. **120:**157–164.
24. **Kazar, J., M. Lesny, P. Propper, D. Valkova, and R. Brezina.** 1993. Comparison of virulence for guinea pigs and mice of different *Coxiella burnetii* phase I strains. Acta Virol. **37:**437–448.
25. **Koster, F. T., J. C. Williams, and J. S. Goodwin.** 1985. Cellular immunity in Q fever: modulation of responsiveness by a suppressor T cell-monocyte circuit. J. Immunol. **135:**1067–1072.
26. **La Scola, B., H. Lepidi, and D. Raoult.** 1997. Pathologic changes during acute Q fever: influence of the route of infection and inoculum size in infected guinea pigs. Infect. Immun. **65:**2443–2447.
27. **Lennette, E. H., W. H. Clark, M. M. Abinanti, O. Brunetti, and J. M. Covert.** 1952. Q fever studies. XIII. The effect of pasteurization on *Coxiella burnetii* in naturally infected milk. Am. J. Hyg. **55:**246–253.
28. **Lesny, M., J. Kazar, P. Propper, and M. Lukacova.** 1991. Virulence and cross-immunity study on guinea pigs infected with different phase I *Coxiella burnetii* strains, p. 666–673. *In* J. Kazar and D. Raoult (ed.), Rickettsiae and rickettsial diseases. Publishing House of the Slovak Academy of Sciences, Bratislava, Slovakia.
29. **Madariaga, M. G., J. Pulvirenti, M. Sekosan, C. D. Paddock, and S. R. Zaki.** 2004. Q fever endocarditis in HIV-infected patients. Emerg. Infect. Dis. **10:**501–504.
30. **Marrie, T. J.** 1990. Acute Q fever, p. 125–160. *In* T. J. Marrie (ed.), Q fever, vol. 1. The disease. CRC Press, Boca Raton, FL.
31. **Marrie, T. J.** 1990. Q fever hepatitis, p. 171–178. *In* T. J. Marrie (ed.), Q fever, vol. 1. The disease. CRC Press, Boca Raton, FL.
32. **Marrie, T. J.** 2004. Q fever pneumonia. Curr. Opin. Infect. Dis. **17:**137–142.
33. **Marrie, T. J., A. Stein, D. Janigan, and D. Raoult.** 1996. Route of infection determines the clinical manifestations of acute Q fever. J. Infect. Dis. **173:**484–487.
34. **Maurin, M., and D. Raoult.** 1999. Q fever. Clin. Microbiol. Rev. **12:**518–553.
35. **McMurray, D. N.** 1994. Guinea pig model of tuberculosis, p. 135–147. *In* B. R. Bloom (ed.), Tuberculosis: pathogenesis, protection, and control. American Society for Microbiology, Washington, DC.
36. **Moos, A., and T. Hackstadt.** 1987. Comparative virulence of intra- and interstrain lipopolysaccharide variants of *Coxiella burnetii* in the guinea pig model. Infect. Immun. **55:**1144–1150.
37. **Ormsbee, R. A.** 1965. Q fever rickettsia, p. 1144–1160. *In* F. L. Horsfall and I. Tamm (ed.), Viral and rickettsial diseases of man. J. B. Lippencott, Philadelphia, PA.
38. Reference deleted.
39. **Penttila, I. A., R. J. Harris, P. Storm, D. Haynes, D. A. Worswick, and B. P. Marmion.** 1998. Cytokine dysregulation in the post-Q-fever fatigue syndrome. QJM **91:**549–560.
40. **Raoult, D., and T. Marrie.** 1995. Q Fever. Clin. Infect. Dis. **20:**489–496.
41. **Raoult, D., A. Raza, and T. J. Marrie.** 1990. Q fever endocarditis and other forms of chronic Q fever, p. 179–120. *In* T. J. Marrie (ed.), Q fever, vol. 1. The disease. CRC Press, Boca Raton, FL.
42. **Roman, M. J., H. A. Crissman, W. A. Samsonoff, K. E. Hechemy, and O. G. Baca.** 1991. Analysis of *Coxiella burnetii* isolates in cell culture and the expression of parasite-specific antigens on the host membrane surface. Acta Virol. **35:**503–510.
43. **Russell-Lodrigue, K. E., G. Q. Zhang, D. N. McMurray, and J. E. Samuel.** 2006. Clinical and pathologic changes in a guinea pig aerosol challenge model of acute Q fever. Infect. Immun. **74:**6085–6091.
44. **Samuel, J. E., M. E. Frazier, and L. P. Mallavia.** 1985. Correlation of

plasmid type and disease caused by *Coxiella burnetii*. Infect. Immun. **49:**775–779.

45. **Scott, G. H., J. C. Williams, and E. H. Stephenson.** 1987. Animal models in Q fever: pathological responses of inbred mice to phase I *Coxiella burnetii*. J. Gen. Microbiol. **133:**691–700.
46. **Stein, A., and D. Raoult.** 1993. Lack of pathotype specific gene in human *Coxiella burnetii* isolates. Microb. Pathog. **15:**177–185.
47. **Stoenner, H. G., R. Holdenried, D. Lackman, and J. S. Orsborn.** 1959. The occurrence of *Coxiella burnetii*, *Brucella*, and other pathogens among fauna of the Great Salt Lake Desert in Utah. Am. J. Trop. Med. Hyg. **8:**590–595.
48. **Stoenner, H. G., and D. B. Lackman.** 1960. The biologic properties of *Coxiella burnetii* isolated from rodents collected in Utah. Am. J. Hyg. **71:**45–51.
49. **Svraka, S., R. Toman, L. Skultety, K. Slaba, and W. L. Homan.** 2006. Establishment of a genotyping scheme for *Coxiella burnetii*. FEMS Microbiol. Lett. **254:**268–274.
50. **Thiele, D., and H. Willems.** 1994. Is plasmid based differentiation of *Coxiella burnetii* in 'acute' and 'chronic' isolates still valid? Eur. J. Epidemiol. **10:**427–434.
51. **Tissot Dupont, H., D. Raoult, P. Brouqui, F. Janbon, D. Peyramond, P. J. Weiller, C. Chicheportiche, M. Nezri, and R. Poirier.** 1992. Epidemiologic features and clinical presentation of acute Q fever in hospitalized patients: 323 French cases. Am. J. Med. **93:**427–434.
52. **Wiegeshaus, E. H., D. N. McMurray, A. A. Grover, G. E. Harding, and D. W. Smith.** 1970. Host-parasite relationships in experimental airborne tuberculosis. 3. Relevance of microbial enumeration to acquired resistance in guinea pigs. Am. Rev. Respir. Dis. **102:**422–429.
53. **Williams, J. C., M. G. Peacock, and T. F. McCaul.** 1981. Immunological and biological characterization of *Coxiella burnetii*, phase I and phase II, separated from host components. Infect. Immun. **32:**840–851.
54. **Zhang, G. Q., and J. E. Samuel.** 2003. Identification and cloning potentially protective antigens of *Coxiella burnetii* using sera from mice experimentally infected with Nine Mile phase I. Ann. N. Y. Acad. Sci. **990:** 510–520.

Editor: R. P. Morrison

Virus Research 144 (2009) 294–297

Contents lists available at ScienceDirect

Virus Research

journal homepage: www.elsevier.com/locate/virusres

Short communication

A novel budgerigar-adenovirus belonging to group II avian adenovirus of *Siadenovirus*

Hiroshi Katoh[a], Kenji Ohya[b], Masahito Kubo[c], Koichi Murata[d], Tokuma Yanai[c], Hideto Fukushi[a,b,*]

[a] Department of Applied Veterinary Sciences, United Graduate School of Veterinary Sciences, Faculty of Applied Biological Sciences, Gifu University, Gifu 501-1193, Japan
[b] Laboratory of Veterinary Microbiology, Faculty of Applied Biological Sciences, Gifu University, Gifu 501-1193, Japan
[c] Laboratory of Veterinary Pathology, Faculty of Applied Biological Sciences, Gifu University, Gifu 501-1193, Japan
[d] Department of Wildlife Science, College of Bioresource Science, Nihon University, Kanagawa 252-0813, Japan

ARTICLE INFO

Article history:
Received 26 February 2009
Received in revised form 16 April 2009
Accepted 16 April 2009
Available online 24 April 2009

Keywords:
Avian adenovirus
Budgerigar
Siadenovirus
Hexon gene
Phylogenetic analysis
Pathology

ABSTRACT

Five budgerigars in the same breeding facility died or showed ruffled feathers. To determine the cause, five dead or euthanized budgerigars were examined. Splenomegaly was observed at necropsy in all birds examined. Histopathology of the spleen revealed a slight-to-moderate deletion of lymphocytes and increase of macrophages. Concurrent congestions in several tissues such as liver, lung, kidney, and/or brain and basophilic intranuclear inclusion bodies in the epithelial cells of renal tubules were found in all the birds examined. Psittacine adenoviral DNA was detected in the kidney of one of the five budgerigars by PCR. Sequencing and phylogenetic analysis of the hexon gene revealed that the adenovirus gene detected in the budgerigar was derived from an unknown adenovirus belonging to the genus *Siadenovirus*. Using a new pair of primers based on the obtained sequence, we confirmed the presence of the newly found adenovirus in all five birds. The newly found unknown adenovirus is designated as Budgerigar Adenovirus 1.

Adenoviruses (AdVs) have been isolated from a wide range of vertebrates including mammals, birds, reptiles, amphibians, and fishes. The classification of adenoviruses of different host species has been recently revised (Benko and Harrach, 2003). Avian adenoviruses are classified into three genera—*Aviadenovirus*, *Atadenovirus*, and *Siadenovirus*. Most of the avian adenoviruses that have been characterized are classified into the genus *Aviadenovirus*, which were previously classified as group I avian adenovirus. Group II turkey adenovirus type 3 (TAdV-3), also named turkey hemorrhagic enteritis virus, was found to be related to members of *Siadenovirus* with frog adenovirus (FrAdV-1) (Davison et al., 2000). In addition, group III egg drop syndrome virus (EDSV) has been moved to the new genera *Atadenovirus* (Benko and Harrach, 1998).

Adenovirus infections in psittacine birds have been identified based on microscopic studies. Infections with adenovirus (Capua et al., 1995) or adenovirus-like particles (Gomez-Villamandos et al., 1995a; Mackie et al., 2003; Mori et al., 1989; Pass, 1987) have been described in a variety of psittacine birds including budgerigars (*Melopsittacus undulatus*), macaws (*Ara* spp.), Amazon parrots (*Amazona* spp.), and cockatoos (*Cacatua* spp.). However, little is known about the genomic organization of adenoviruses infecting psittacine birds. Recently, adenovirus was detected by PCR in Senegal parrots (*Poicephalus senegalus*) showing clinical and pathological signs of adenovirus infection and was identified by its hexon gene sequence as a new avian adenovirus belonging to *Aviadenovirus* (Raue et al., 2005). Designation of this virus as psittacine adenovirus (PsAdV) was approved by the International Committee on Taxonomy of Viruses (ICTV) (Raue et al., 2005).

The hexon protein is the major viral capsid protein of adenovirus (Norrby et al., 1969). The hexon protein consists of two functional components: the conserved pedestal regions P1 and P2 and the variable loops L1–L4 (Athappilly et al., 1994; Roberts et al., 1986). L1, L2 and L4 are located at the surface of the hexon protein and interact with the immune response of the host. Thus, the hexon protein is known to possess family-, genus-, species-, and type-specific determinants, which has seven hypervariable regions (HVR) in the L regions (Crawford-Miksza and Schnurr, 1996; Li et al., 1997). The hexon gene has been used for the phylogenetic study of adenoviruses (Davison et al., 2000; Kovacs et al., 2003).

In the present study, we examined adenovirus infection in budgerigars having intranuclear inclusion bodies in the kidneys. Genomic adenovirus DNA was detected in the examined bird tissues by PCR. The adenovirus found in this study represents a new adenovirus in the family *Siadenovirus* that is similar to TAdV-3

* Corresponding author at: Laboratory of Veterinary Microbiology, Faculty of Applied Biological Sciences, Gifu University, Yanagido 1-1, Gifu 501-1193, Japan. Tel.: +81 58 293 2946; fax: +81 58 293 2946.
E-mail address: hfukushi@gifu-u.ac.jp (H. Fukushi).

0168-1702/$ – see front matter © 2009 Elsevier B.V. All rights reserved.
doi:10.1016/j.virusres.2009.04.012

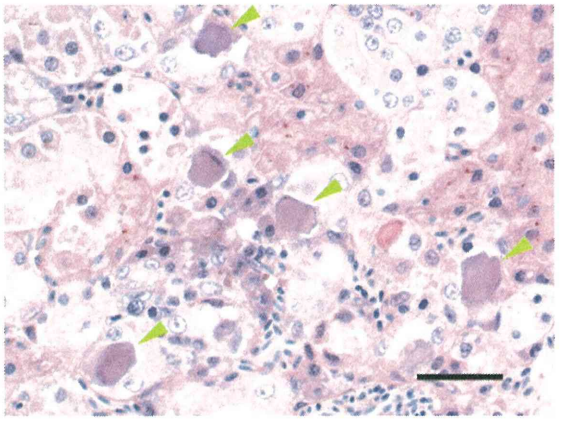

Fig. 1. Histological section of the kidney of Bird 1. Basophilic intranuclear inclusion bodies were indicated by arrow heads. Hematoxylin and eosin stain; bar = 25 μm.

and FrAdV-1 based on a phylogenetic analysis of the amino acid sequences of the hexon gene.

We examined five budgerigars that were housed together in the same breeding facility. Of the five examined birds, one (Bird 1) with ruffled feathers was euthanized. The other four budgerigars (Birds 2–5) died with no clinical symptoms. Postmortem examination was carried out on Birds 1–3 but not Birds 4 and 5 because the bodies had decomposed. At necropsy, splenomegaly was observed in Birds 2 and 3. A histopathological study of the spleen revealed a slight-to-moderate deletion of lymphocytes and an increase of macrophages. All three birds (Birds 1–3) also had concurrent congestions in several tissues such as liver, lung, kidney, and/or brain. Aggregates of inflammatory cells were observed in their livers and kidneys. In addition, diffused necrosis was observed in the liver and spleen of Bird 1. Basophilic intranuclear inclusion bodies were found in the epithelial cells of renal tubules of all three birds (Fig. 1).

A histopathological examination revealed basophilic intranuclear inclusion bodies, suggesting that these birds were infected by adenovirus. In order to detect adenoviral genomic DNA, PCR was performed using primers designed to amplify the L1 region of the hexon gene of fowl adenovirus (FAdV) and PsAdV as described previously (Raue et al., 2005). DNA was extracted from 50 mg of liver, spleen, and kidney with a SepaGene nucleic acid extraction kit (Sanko Junyaku Co., Tokyo, Japan) according to the manufacturer's instructions. DNA was finally dissolved in 25 μl of Tris–EDTA (10 mM Tris–HCl, 1 mM EDTA; pH 8.0) and stored at −30 °C until use.

We were able to amplify the hexon gene from the kidney of Bird 2 (Fig. 2A), indicating the presence of adenoviral DNA. The PCR products were cloned and sequenced as described previously (Ogawa et al., 2005). The partial hexon gene sequence obtained was deposited in GenBank with GenBank accession no. AB485763. The nucleotide sequence is 528 bp in length and encodes 176 amino acids. Compared with the published adenovirus sequences, the sequence shared the highest amino acid sequence identity with that of raptor adenovirus grouped into *Siadenovirus* (60.5%) (Table 1). Therefore, we concluded that the sequence was derived from an adenovirus infecting the budgerigar. The adenovirus was designated as budgerigar adenovirus 1 (BuAdV-1). The analysis revealed a similarity of 29.4–35.0% to the deduced amino acid sequences obtained from the FAdV and PsAdV reference strains, which are representatives of *Aviadenovirus* (data not shown). In contrast, the deduced amino acid sequence of BuAdV-1 showed 53.7% and 44.5% homologies to the sequences of the *Siadenovirus* TAdV-3 and FrAdV-1, respectively. The adenovirus that had the lowest homology to BuAdV-1 (24.4%) was EDSV.

To determine whether the other four birds were infected with BuAdV-1, a new pair of primers, BAV-F (5′-aaccatctcccaatacaggt-3′) and BAV-R (5′-aaccatctcccaatacaggt-3′), was designed based on the sequence of the hexon gene of BuAdV determined in this study. The expected fragment size was approximately 200 bp. PCR was carried out using 1.25 units of TaKaRa *Ex Taq* (TaKaRa Bio Inc., Shiga, Japan) in a 50 μl reaction. The PCR program consisted of primary denaturation at 94 °C for 5 min, 35 cycles with denaturation at 94 °C for 30 s, annealing at 54 °C for 30 s, and extension at 72 °C for 30 s, followed by a final extension at 72 °C for 5 min. As a result, viral DNA was detected in the kidney of all five birds (Fig. 2B), indicating that each was infected with BuAdV-1. This result indicates that it is necessary to consider the presence of unknown adenoviruses belonging to not only *Aviadenovirus* but also other genera of adenovirus including *Siadenovirus* for epidemiological and etiological studies of adenovirus infection in psittacine birds.

To confirm the taxonomic position of the BuAdV-1, a phylogenetic tree of the deduced amino acid sequences of the hexon protein from 11 avian adenoviruses, one reptilian adenovirus, and one fish adenovirus was constructed by the UPGMA method (Fig. 3). The 13 adenoviruses can be divided into four clusters as described by other researchers (Kovacs et al., 2003). BuAdV-1 belongs to the genus *Siadenovirus* not to *Aviadenovirus*. Similarly, other phylogenetic analyses including the Neighbour-joining method, maximum parsimony analysis, and maximum likelihood approach showed that the BuAdV-1 sequence clustered within *Siadenovirus* (data not shown). These results suggest that BuAdV-1 is genetically related to raptor adenovirus 1 and TAdV-3, which were included in *Siadenovirus*. *Siadenovirus* was recently proposed as the fourth adenovirus genus (Davison et al., 2000).

Diseases caused by adenovirus belonging to group II, such as hemorrhagic enteritis of turkeys, marble spleen disease of pheasants, and avian adenosplenomegaly of chicken, have been reported in several avian species (Shivaprasad, 2008). Group II adenovirus infections were also reported in psittacine birds but not in budgerigars. However, no genetic investigation was carried out in these psittacine birds (Gomez-Villamandos et al., 1995a,b). Previous studies (Capua et al., 1995; Weissenbock and Fuchs, 1995) observed

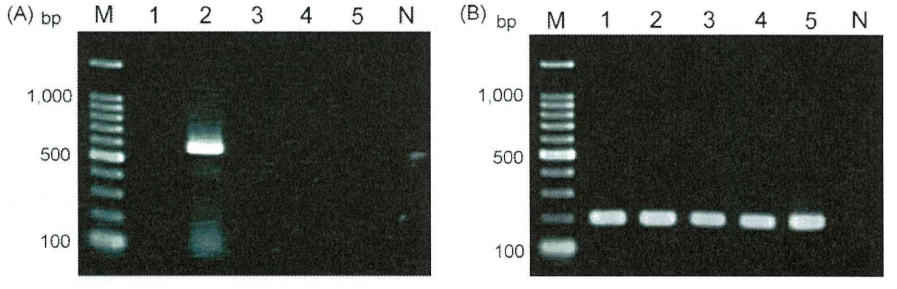

Fig. 2. Demonstration of the presence of adenoviral DNA in kidney samples using the hexon based primer pair (A) Hex L1-s/Hex L1-as (Raue et al., 2005) and (B) BAV-F/BAV-R. Lane 1, Bird 1; 2, Bird 2; 3, Bird 3; 4, Bird 4; 5, Bird 5; N, negative control (D_2W); M, 100 bp DNA Ladder (ToYoBo, Osaka, Japan).

Table 1
Adenovirus strains used in this study.

Genus	Genotype	Virus name	Host	Accession no.
Aviadenovirus	A	FAdV strain CELO	Chicken (*Gallus gallus*)	AF339914
	B	FAdV strain 340	Chicken (*G. gallus*)	AF508952
	C	FAdV strain KR5	Chicken (*G. gallus*)	AF508951
	D	FAdV strain SR49	Chicken (*G. gallus*)	AF508948
	E	FAdV strain 764	Chicken (*G. gallus*)	AF508958
		PsAdV	Senegal parrot (*Poicephalus senegalus*)	AY852270
		Northern aplomado falcon adenovirus	Northern aplomado falcon (*Falco femoralis septentrionalis*)	AAV90966
Siadenovirus		TAdV-3	Turkey (*Meleagris gallopavo*)	AF075681
		Raptor adenovirus	Harris hawk (*Parabuteo unicinctus*)	EU715130
		FrAdV-1	Frog	AF224336
Atadenovirus		EDSV	Chicken (*G. gallus*)	Y09598
Unclassified genus		White strugeon adenovirus	White sturgeon (*Acipenser transmontanus*)	AJ495768

intranuclear inclusion bodies in lymphocytes, severe increases in the mononuclear phagocytic system cells, and lymphoid depletion of spleen in group II adenovirus infections. However, most adenovirus infections in psittacine birds including PsAdV infection reported were associated with necrotizing hepatitis and basophilic intranuclear inclusion bodies in hepatocytes. Group II avian adenoviruses have also been associated with hemorrhagic enteritis, lung edema, and splenomegaly (Massi et al., 1995). Although no intranuclear inclusion bodies were found in the spleen and no hemorrhagic enteritis was found in the intestines, the histopathological characteristics of the examined cases are consistent with those reported for group II avian adenovirus infections.

Because embryonated budgerigar eggs were not available, attempts to isolate BuAdV-1 using primary chicken embryo fibroblast cells failed (data not shown). Group II avian adenoviruses are reported to be difficult to isolate with cell culture (Nazerian and Fadly, 1987). Successful isolation is required for further virological characterization.

In conclusion, histopathological and genetic investigations revealed that BuAdV-1 found in the present study is a

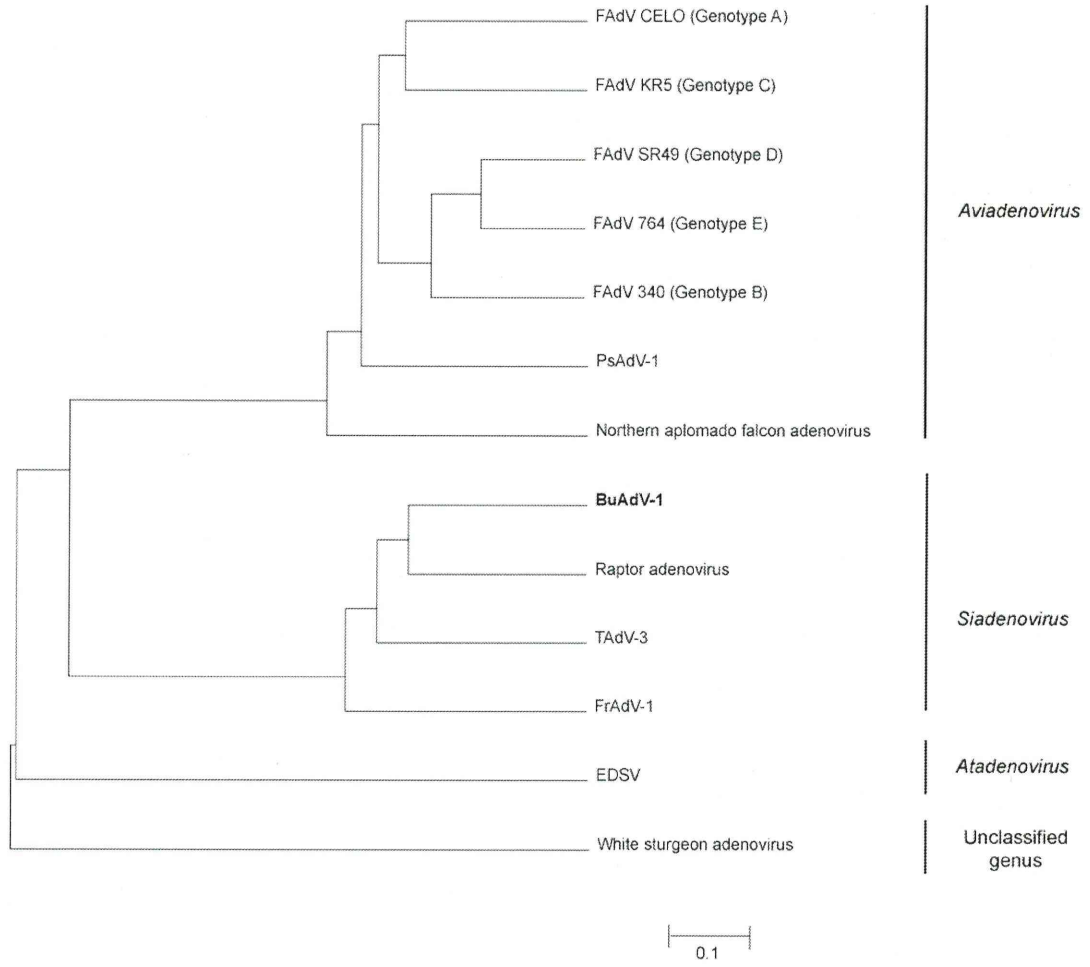

Fig. 3. Phylogenetic analysis of BuAdV-1 and other reference strains based on the L1 region of the hexon gene. The tree was obtained using the UPGMA method with the Genetyx-Mac version 14.0.0 computer software. Typing of FAdV into genogroups (A–E) according to Zsak and Kisary (1984) is shown in parentheses.

new adenovirus and belongs to group II avian adenovirus of *Siadenovirus*.

References

Athappilly, F.K., Murali, R., Rux, J.J., Cai, Z., Burnett, R.M., 1994. The refined crystal structure of hexon, the major coat protein of adenovirus type 2, at 2.9 A resolution. J. Mol. Biol. 242 (4), 430–455.

Benko, M., Harrach, B., 1998. A proposal for a new (third) genus within the family *Adenoviridae*. Arch. Virol. 143 (4), 829–837.

Benko, M., Harrach, B., 2003. Molecular evolution of adenoviruses. Curr. Top. Microbiol. Immunol. 272, 3–35.

Capua, I., Liberti, L., Gough, R.E., Casaccia, C., Asdrubali, G., 1995. Isolation and characterization of an adenovirus associated with inclusion body hepatitis in psittacine birds. Avian Pathol. 24 (4), 717–722.

Crawford-Miksza, L., Schnurr, D.P., 1996. Analysis of 15 adenovirus hexon proteins reveals the location and structure of seven hypervariable regions containing serotype-specific residues. J. Virol. 70 (3), 1836–1844.

Davison, A.J., Wright, K.M., Harrach, B., 2000. DNA sequence of frog adenovirus. J. Gen. Virol. 81 (Pt 10), 2431–2439.

Gomez-Villamandos, J.C., Bautista, M.J., Carrasco, L., Hervas, J., Sierra, M.A., 1995a. Electron microscopic evidence for infection of splenic dendritic cells by adenovirus in psittacine birds. Res. Virol. 146 (6), 389–395.

Gomez-Villamandos, J.C., Muias, J.M., Hervas, J., De Lara, F.C., Perez, J., Mozos, E., 1995b. Spleno-enteritis caused by adenovirus in psittacine birds: a pathological study. Avian Pathol. 24 (3), 553–563.

Kovacs, G.M., LaPatra, S.E., D'Halluin, J.C., Benko, M., 2003. Phylogenetic analysis of the hexon and protease genes of a fish adenovirus isolated from white sturgeon (*Acipenser transmontanus*) supports the proposal for a new adenovirus genus. Virus Res. 98 (1), 27–34.

Li, Q.G., Lindman, K., Wadell, G., 1997. Hydropathic characteristics of adenovirus hexons. Arch. Virol. 142 (7), 1307–1322.

Mackie, J.T., Black, D., Prior, H., 2003. Enteritis associated with adenovirus-like particles in captive lorikeets. Aust. Vet. J. 81 (5), 293–295.

Massi, P., Gelmetti, D., Sironi, G., Dottori, M., Lavazza, A., Pascucci, S., 1995. Adenovirus-associated haemorrhagic disease in guinea fowl. Avian Pathol. 24 (2), 227–237.

Mori, F., Touchi, A., Suwa, T., Itakura, C., Hashimoto, A., Hirai, K., 1989. Inclusion bodies containing adenovirus-like particles in the kidneys of psittacine birds. Avian Pathol. 18 (1), 197–202.

Nazerian, K., Fadly, A.M., 1987. Further studies on in vitro and in vivo assays of hemorrhagic enteritis virus (HEV). Avian Dis. 31 (2), 234–240.

Norrby, E., Marusyk, H., Hammarskjold, M.L., 1969. The relationship between the soluble antigens and the virion of adenovirus type 3. V. Identification of antigen specificities available at the surface of virions. Virology 38 (3), 477–482.

Ogawa, H., Yamaguchi, T., Fukushi, H., 2005. Duplex shuttle PCR for differential diagnosis of budgerigar fledgling disease and psittacine beak and feather disease. Microbiol. Immunol. 49 (3), 227–237.

Pass, D.A., 1987. Inclusion bodies and hepatopathies in psittacines. Avian Pathol. 16 (4), 581–597.

Raue, R., Gerlach, H., Muller, H., 2005. Phylogenetic analysis of the hexon loop 1 region of an adenovirus from psittacine birds supports the existence of a new psittacine adenovirus (PsAdV). Arch. Virol. 150 (10), 1933–1943.

Roberts, M.M., White, J.L., Grutter, M.G., Burnett, R.M., 1986. Three-dimensional structure of the adenovirus major coat protein hexon. Science 232 (4754), 1148–1151.

Shivaprasad, H.L., 2008. Adenovirus group II-like infection in chukar partridges (*Alectoris chukar*). Avian Dis. 52 (2), 353–356.

Weissenbock, H., Fuchs, A., 1995. Histological and ultrastructural characterisation of hepatic intranuclear inclusion bodies in psittacine birds and pigeons. Avian Pathol. 24 (3), 507–521.

Zsak, L., Kisary, J., 1984. Grouping of fowl adenoviruses based upon the restriction patterns of DNA generated by BamHI and HindIII. Intervirology 22 (2), 110–114.

Veterinary Microbiology 138 (2009) 69–77

Contents lists available at ScienceDirect

Veterinary Microbiology

journal homepage: www.elsevier.com/locate/vetmic

Molecular characterization of avian polyomavirus isolated from psittacine birds based on the whole genome sequence analysis

Hiroshi Katoh [a], Kenji Ohya [b], Yumi Une [c], Tsuyoshi Yamaguchi [a,b,1], Hideto Fukushi [a,b,*]

[a] Department of Applied Veterinary Sciences, United Graduate School of Veterinary Sciences, Japan
[b] Laboratory of Veterinary Microbiology, Faculty of Applied Biological Sciences, Gifu University, Gifu 501-1193, Japan
[c] Laboratory of Veterinary Pathology, Azabu University, Kanagawa 229-8501, Japan

ARTICLE INFO

Article history:
Received 9 September 2008
Received in revised form 16 February 2009
Accepted 2 March 2009

Keywords:
Adaptation
Amino acid deletion
Avian polyomavirus (APV)
Sequence analysis
VP4

ABSTRACT

Seven avian polyomaviruses (APVs) were isolated from seven psittacine birds of four species. Their whole genome sequences were genetically analyzed. Comparing with the sequence of BFDV1 strain, nucleotide substitutions in the sequences of seven APV isolates were found at 63 loci and a high level of conservation of amino acid sequence in each viral protein (VP1, VP2, VP3, VP4, and t/T antigen) was predicted. An A-to-T nucleotide substitution was observed in non-control region of all seven APV sequences in comparison with BFDV1 strain. Two C-to-T nucleotide substitutions were also detected in non-coding regions of one isolate. A phylogenetic analysis of the whole genome sequences indicated that the sequences from the same species of bird were closely related. APV has been reported to have distinct tropism for cell cultures of various avian species. The present study indicated that a single amino acid substitution at position 221 in VP2 was essential for propagating in chicken embryonic fibroblast culture and this substitution was promoted by propagation on budgerigar embryonic fibroblast culture. For two isolates, three serial amino acids appeared to be deleted in VP4. However, this deletion had little effect on virus propagation.

1. Introduction

Avian polyomavirus (APV) was first characterized as a pathogen in young budgerigars (*Melopsittacus undulatus*) in the early 1980s (Davis et al., 1981), and was subsequently designated budgerigar fledgling disease virus (Bernier et al., 1981; Bozeman et al., 1981). Although the virus was designated budgerigar fledgling disease polyomavirus by the International Committee on Taxonomy of Viruses, it is now called APV because of its broad host range (Johne and Muller, 2007).

APV infection is characterized by hepatitis, ascites, and hydropericardium as the main clinical symptoms and has a mortality rate of up to 100% in fledglings (Kaleta et al., 1984; Krautwald et al., 1989). APV infections have also been detected in other psittacine species, causing clinical signs similar to those observed in budgerigars, although the degree of susceptibility to and the severity of the disease seem to vary among species (Enders et al., 1997).

The APV virion is icosahedral and nonenveloped with a diameter 45–50 nm (Bozeman et al., 1981). The genome is a circular double-stranded DNA, 4981 bp in size forming a chromosome-like structure with cellular histones (Rott et al., 1988). Functionally the APV genome can be divided into early and late gene coding regions. The early region of APV encodes a large tumor antigen and a small tumor

* Corresponding author at: Laboratory of Veterinary Microbiology, Faculty of Applied Biological Sciences, Gifu University, Gifu 501-1193, Japan. Tel.: +81 58 293 2946; fax: +81 58 293 2946.
E-mail address: hfukushi@gifu-u.ac.jp (H. Fukushi).
[1] Present address: Avian Zoonosis Research Center, Faculty of Agriculture, Tottori University, Tottori 680-8553, Japan.

0378-1135/$ – see front matter © 2009 Elsevier B.V. All rights reserved.
doi:10.1016/j.vetmic.2009.03.007

antigen by analogy with mammalian polyomaviruses. The late region in APV encodes a major structural protein, VP1, and two minor structural proteins, VP2 and VP3. VP4 is regularly observed in virus particles in addition to the structural proteins VP1-3 (Johne and Muller, 2001). VP4 has a molecular weight of 32 kDa and is unique to APV and not found among the most closely related mammalian polyomaviruses that infect humans, monkeys, mice, and hamsters. VP4 is essential for APV replication and interacts with VP1 as well as with viral double-stranded DNA (Johne and Muller, 2001). Recently, an additional protein, consisting of the 125 C-terminal amino acid residues of VP3, has been identified in simian virus 40 (SV40)-infected cells (Daniels et al., 2007). SV40 is a mammalian polyomavirus that was detected in African green monkeys in 1960. Although this protein of SV40 has no similarities regarding sequence, structure, or biological properties with VP4 of APV, it has also been designated VP4.

Although mammalian polyomaviruses are largely species-specific and infect only one or a few closely related species, APV can replicate in cultured cells prepared from a variety of avian species; e.g. budgerigar, chicken, Muscovy duck, and quail (Stoll et al., 1993, 1994). Host restriction of APV has been reported to be due to a single amino acid at position 221 in the common region of VP2/VP3 (Stoll et al., 1994).

Despite the presence of APV infections in several species of psittacine birds in many countries including Canada (Bernier et al., 1981), Japan (Hirai et al., 1984; Ogawa et al., 2006), Australia (Pass, 1985), Germany (Stoll et al., 1993), Slovakia (Literak et al., 2006), and Taiwan (Hsu et al., 2006), APV isolates from different species of birds and geographical origins are closely related to each other and can be grouped into one genotype as well as one serotype (Johne and Muller, 1998; Khan et al., 2000; Phalen et al., 1999). However, to date, APV sequence information was limited to only four whole genome sequences and partial genome sequence analysis (Johne and Muller, 1998; Ogawa et al., 2006; Phalen et al., 1999; Rott et al., 1988; Stoll et al., 1993). To understand how APV differs from mammalian polyomaviruses in structure and virus–host relationships, it is necessary to analyze the genomes of additional strains of APV. The present study was conducted to investigate the genetic diversity of APV isolated from seven psittacine birds that died in Japan from 2003 to 2006.

2. Materials and methods

2.1. Specimens

Seven bird samples obtained in routine diagnostic procedures in our laboratory from 2003 to 2006 were investigated in this study. Each of them was derived from different aviaries or owners except Birds 1 and 2, which were from the same breeding aviary. Each bird was checked for the presence of pathogen-specific DNA common with psittacine birds such as APV, beak and feather disease virus, psittacid herpesvirus, and *Chlamydophila psittaci* by PCR (Chahota et al., 2006; Ogawa et al., 2005; Tomaszewski et al., 2001). APV-specific DNA was detected in each bird. No other pathogens were detected. Each bird also appeared to have the symptoms of APV infection. Bird species, case histories, DNA detection, and pathological findings of each bird are summarized in Table 1.

2.2. Cells and viruses

Budgerigar embryonic fibroblast (BEF) and chicken embryonic fibroblast (CEF) primary cultures were prepared using standard techniques and maintained in Eagle's minimum essential medium supplemented with 5% fatal bovine serum. Hy-line Julia chicken strain was used for preparation of CEF culture. APV GFM-1, a strain that was isolated from budgerigar in our laboratory in 1982 (Hirai et al., 1984), was used for comparison with the viruses in this study.

2.3. DNA extraction

DNA was extracted from 50 mg of liver tissues and 10^5 infected cells with a SepaGene nucleic acid extraction kit (Sanko Junyaku Co., Tokyo, Japan) according to the manufacturer's instructions. DNA was finally dissolved in 25 μl of Tris–EDTA (10 mM Tris–HCl, 1 mM EDTA; pH 8.0) and stored at −30 °C until use.

2.4. RNA extraction and reverse transcription-PCR (RT-PCR)

Total RNA was isolated from 10^5 CEF cells inoculated with APV using TRIzol RNA extraction reagent (Invitrogen, California, U.S.A.) following the manufacturer's instructions. RNA was finally dissolved in 20 μl of RNase free water and stored at −80 °C until use.

Extracted total cellular RNA (1 μg) was dissolved with DNaseI (Invitrogen) and heated at 65 °C for 5 min. To synthesize the first strand of cDNA, RT reaction was performed in a total volume of 20 μl reaction mixture containing 100 units of Rever Tra Ace reverse transcriptase (ToYoBo Co., Osaka, Japan), reaction buffer containing 50 mM Tris–HCl (pH 7.5), 400 μM of each dATP, dCTP, dGTP, and dTTP, 25 pmoles of random primers (9 mer), 20 units of RNase Inhibitor (ToYoBo Co.), and template RNA. RT reaction program consisted of annealing at 30 °C for 10 min and extension at 42 °C for 20 min, followed by enzyme inactivation at 70 °C for 10 min.

PCR was carried out in a total volume of 50 μl reaction mixture containing 1.25 units of TaKaRa *Ex Taq* (TaKaRa Bio, Inc., Shiga, Japan), 2 mM of Mg^{2+} in buffer, 200 μM of each dATP, dCTP, dGTP, and dTTP, 0.25 μM of each primer (VP4-F: 5′-TCATCCAGCGCGAGAT-3′; VP4-R: 5′-CCGATGTCCCTGAATATA-3′) designed from the sequence of the BFDV1 strain (Rott et al., 1988) that was subsequently corrected by Stoll et al. (1993), and 2 μg of template cDNA. The PCR program consisted of primary denaturation at 94 °C for 5 min, 35 cycles with denaturation at 94 °C for 30 s, annealing at 46 °C for 30 s, and extension at 72 °C for 30 s, followed by a final extension at 72 °C for 5 min. The PCR products were separated on 2% agarose gels and visualized by staining with ethidium bromide.

Table 1
Specimen data and case histories in this study and results of APV DNA detection in original liver sample as well as of virus isolation.

Bird no.	Species	Sex	Age (months)	Origin (prefecture)	Date of death	Clinical signs	Detection of APV DNA in liver sample	Gross pathology	Histopathology	CPE in cell cultures		Strain
										CEF	BEF	
1	Black-headed caique (*Pionites melanocephala*)	M	3	Kanagawa	July, 2003	Thinness, weakness, ataxia, convulsion	Detected	Depilate, edematous changes of brain, hemorrhage of epicardium	Vacuolation of neurons, hepatic necrosis, splenic necrosis	–	+	APV1
2	Black-headed caique (*Pionites melanocephala*)	M	2.5	Kanagawa	July, 2003	Ataxia	Detected	Depilate, ascites	Vacuolation of neurons, edematous changes of perineurons	–	+	APV2
3	Eclectus parrot (*Eclectus roratus*)	F	Unknown	Aichi	April, 2004	Vomiting	Detected	Hepatomegaly, splenomegaly, swollen kidneys	Meningitis, hepatitis, bronchitis, interstitial nephritis	–	–	APV3
4	Black-headed Caique (*Pionites melanocephala*)	Unknown	2	Kanagawa	April, 2005	Vomiting weakness	Detected	NT	NT	–	+	APV4
5	Black-headed caique (*Pionites melanocephala*)	Unknown	2	Kanagawa	April, 2005	Vomiting weakness	Detected	NT	NT	–	+	APV5
6	Ducorp's cockatoo (*Cacatua ducorpsii*)	M	Unknown	Tokyo	July, 2005	No obvious lesion	Detected	No obvious lesion	Inclusion bodies in liver, lung congestion	–	+	APV6
7	White-bellied caique (*Pionites leucogaster*)	M	5	Tokyo	January, 2006	Runny nose coughing, melena	Detected	Hemopericardium, pale liver, splenomegaly	Hepatic necrosis, bronchitis	+	+	APV7

NT indicates that pathological examination was not performed because of decomposition. M indicates male. F indicates female. Plus indicates that CPE was observed. Minus indicates that no CPE was observed.

2.5. Virus isolation and virus inoculation

A 10% (w/v) suspension of liver from each bird was prepared in cell-culture medium and centrifuged at 1000 × *g* for 10 min at 4 °C. CEF and BEF cultures in 24-well culture plates were inoculated with 0.1% diluted supernatant, respectively. After incubation at 39 °C for 60 min to allow virus absorption, the inoculated cultures were incubated at 39 °C (first passage). The inoculated cultures were observed for cytopathic effect (CPE) daily for 1 week. Thereafter, inoculated cultures were disrupted by three cycles of freezing and thawing and centrifuged at 1000 × *g* for 10 min at 4 °C. Supernatant was inoculated onto prepared fresh cultures (second passage). All cultures were passaged in this way three times, whenever CPE was observed at first or second passage.

2.6. Sequence analysis of whole APV genome

PCR was performed for amplification of APV genome from seven isolates and the GFM-1 strain. One pair of primers (APV-AF: 5′-ACAATGCCTAACGGAACGCC-3′, positions 375–395; APV-AR: 5′-CACCGAAGCGGCGATACTATA-3′, positions 3624–3604) was used to amplify an approximately 3 kbp fragment of the APV genome. Another pair of primers (APV-BF: 5′-GAGGCCTACCACGCTATTTCAGTA-3′, positions 2710–2733; APV-BR: 5′-GCACTTAGCGCCTGTC-CAAT-3′, positions 1230–1211) was used to amplify another approximately 3 kbp fragment. Oligonucleotide positions refer to the sequence of the BFDV1 strain. PCR was carried out in a total volume of 50 μl reaction mixture containing 2.5 units of TaKaRa *LA Taq* (TaKaRa Bio, Inc.), 2.5 mM of Mg^{2+} in buffer, 400 μM of each dATP, dCTP, dGTP, and dTTP, 0.25 μM of each primer, and 2 μg of template DNA. The PCR program consisted of primary denaturation at 94 °C for 5 min, 35 cycles with denaturation at 94 °C for 1 min, annealing at 60 °C for 1 min, and extension at 72 °C for 4 min, followed by a final extension at 72 °C for 10 min. PCR products were precipitated using 2.5 volumes of 99.5% ethanol and 0.3 M sodium acetate (pH 5.2), washed once with 70% ethanol, dried and resuspended in 25 μl of Tris–EDTA.

Two fragments were sequenced by the primer walking method. The primers used are shown in Table 2. The genome sequences were assembled using the phredPhrap and consed programs (Ewing and Green, 1998; Ewing et al., 1998). For sequence comparison, the genome sequences of four APV were obtained from the following GenBank accessions: strain BFDV (AF118150); strain BFDV1 (AF241168); strain BFDV4 (AF241169); strain BFDV5 (AF241170). In addition, the 48 partial sequences (AB241069–AB241073, AF054335–AF054418, DQ304717–DQ304767, and DQ074760–DQ074761) were also obtained from GenBank. Multiple alignment was performed using Genetyx-Mac version 14.0.0 computer software (Genetyx Co., Ltd,. Tokyo, Japan). The sequences of APV1–7 and GFM-1 have been submitted to GenBank and have been given accession numbers AB453159–AB453166 and AB477106.

A phylogenetic tree was obtained using the neighbor-joining method with Genetyx-Mac version 14.0.0 computer software (Saitou and Nei, 1987) and displayed, and plotted using the Njplot program (Galtier et al., 1996). The Bootstrap values were calculated to evaluate the topological accuracy of each tree by taking 1000 random samples from the multiple alignment (Felsenstein, 1985).

2.7. Titration of viral infectivity

To compare viral growth in CEF culture, the supernatant and cells were collected at 12, 24, 36, 48, 60, 72, 96, and 120 h post-infection (h.p.i.) at a multiplicity of infection (MOI) of 0.1. The cells were frozen and thawed three times

Table 2
Primers used for primer walking sequencing.

Primers	Sequence (5′-3′)	Location (region)	Origin (reference)
APV-1s	ACAATGCCTAACGGAACGCC	375–395 (VP4)	This study
APV-1as	GGCGTTCCGTTAGGCATTGT	395–375 (VP4)	NC1 (Phalen et al., 1999)
APV-2s	CACCGAGACAACCGGCCCTA	890–910 (VP4)	This study
APV-2as	TAGGGCCGGTTGTCTCGGTG	910–890 (VP4)	This study
APV-3as	GCACTTAGCGCCTGTCCAAT	1230–1211 (VP2)	This study
APV-3s	TTAGAAACCGCACGTTGGA	1541–1560 (VP2/VP3)	VP2/3-2 (Phalen et al., 1999)
APV-4as	TCCAACGTGCGGTTTCTAA	1560–1541 (VP2/VP3)	This study
APV-4s	CCAGGAGGTGCAATGCAACG	1790–1809 (VP2/VP3)	This study
APV-5as	CGTTGCATTGCACCTCCTGG	1809–1790 (VP2/VP3)	VP2/3-3 (Phalen et al., 1999)
APV-5s	CTTATGTGGGAGGCTGCAGTGTT	2182–2207 (VP1)	VP1-1 (Phalen et al., 1999)
APV-6as	AACACTGACAGCCTCCCACATAAG	2207–2182 (VP1)	This study
APV-6s	GGGCTACAAGGCCCGACTAG	2444–2463 (VP1)	This study
APV-7s	GAGGCCTACCACGCTATTTCAGTA	2710–2733 (VP1)	This study
APV-7as	TACTGAAATAGCGTGGTAGGCCTC	2733–2710 (VP1)	VP1-2 (Phalen et al., 1999)
APV-8s	TCGAGGTTTACGGGTACACT	3342–3361 (T-antigen)	This study
APV-8as	AGTGTACCCGTAAACCTCGA	3361–3342 (T-antigen)	T-ag-1 (Phalen et al., 1999)
APV-9s	TATAGTATCGCCGCTTCGGTG	3604–3624 (T-antigen)	This study
APV-9as	CACCGAAGCGGCGATACTATA	3624–3604 (T-antigen)	T-ag-2 (Phalen et al., 1999)
APV-10as	CCGGACTGTGCTACGTAACATTC	3748–3770 (T-antigen)	T-ag-3 (Phalen et al., 1999)
APV-10s	CGTCGATATACGCGTCGGTT	4241–4260 (T-antigen)	T-ag-4 (Phalen et al., 1999)
APV-11as	AATCAGGGCAGCTCTGCACG	4260–4241 (T-antigen)	This study
APV-12as	CGTGCAGAGCTGCCCTGATT	4390–4409 (T-antigen)	T-ag-5 (Phalen et al., 1999)
APV-11s	TTCAGTGCCGTGCGACG	4887–4903 (t/T-antigen)	T-ag-6 (Phalen et al., 1999)
APV-13as	CGTCGCACGGCACTGAA	4903–4887 (t/T-antigen)	This study

to release cell-associated viruses. The virus titer was determined by 50% tissue culture infectious dose ($TCID_{50}$) assay using CEF culture. A limiting dilution method combined with CPE was applied for the determination of infectivity. The data of three independent experiments were averaged, expressed as mean ± SD, and compared between the two titers using Student's *t*-test. A P value <0.01 was considered as significant.

3. Results

3.1. Virus isolation

Chicken embryonic fibroblast (CEF) primary culture was used to isolate viral agents in our routine diagnosis. Although six samples were negative over all passages in CEF culture, one sample (Bird 7) showed CPE after the third passage (Table 1). The results of PCR and pathological examination indicated that these birds were infected with APV. BEF culture was used to enhance the isolation efficiency. Six samples (Birds 1, 2, 4, 5, 6, and 7) showed CPE in the first or second passage in BEF culture. CPE was characterized by swelling of the nuclei, vacuolization of the cytoplasm, and gradual detachment of the cells from the substrate in both cell cultures. We tried to adapt each virus isolates in BEF culture to CEF culture because only a few budgerigar embryos were available for preparation of the cultures. After three passages in BEF culture, all isolates were adapted to propagate on CEF culture.

3.2. Sequence analysis of whole genome DNA

The whole genome sequences of seven APV isolates were determined. The lengths of APV1 and APV2 were 4971 bp and the lengths of the others were 4981 bp. The percentages of nucleotide substitutions were determined by comparison with the BFDV1 sequence. Excluding deletions, all seven sequences were found to be closely related to each other at the nucleotide level, showing 0.4% to 0.7% variation. Nucleotide substitutions were found at 63 loci including 24 amino acid substitutions in the 7 sequences in this study (Tables 3 and 4).

The predicted number of amino acid substitutions ranged from 0.0 to 0.6% for VP1, 0.6 to 2.1% for VP2, 0.9 to 3.0% for VP3, and 0.5% for T-antigen (Table 4). The variations in amino acid sequence in VP4, not counting the deletions in APV1 and APV2, were 0.0–0.6%. None of the sequences had any amino acid substitutions in the t-antigen. An amino acid substitution in VP2 (R234H) was unique to the sequences of APV1, APV2, APV4, and APV5, which were derived from black-headed caiques (*Pionites melanocephala*) compared with 12 APV complete genome sequences.

C-to-T nucleotide substitutions were detected in non-coding control regions in APV7 (positions 123 and 2945). Unlike BFDV1, all seven APV sequences in this study had an A-to-T nucleotide substitution at position 34, which is not in a control region. No other nucleotide changes were observed in these regions, the putative replication origin (positions 8–60), or the transcriptional control region (positions 80–126 and 131–176). The AATAAA motifs at positions 2971–2966 (the early mRNA polyadenylation signal) and 2979–2984 (the late mRNA polyadenylation signal) were conserved in all sequences in this study.

A 9-bp serial deletion and a 1-bp deletion were detected in the VP4 regions of APV1 and APV2 (Fig. 1). Because two introns are removed from the early mRNA of VP4, the matured mRNA of VP4 consists of 531 bases: 176 amino acids plus a stop codon (Luo et al., 1995). There is a 9-bp deletion close to the splicing position and 1-bp deletion inside the first intron.

3.3. Phylogenetic analysis of APV whole genome sequences

In a phylogenetic tree based on the whole genome sequences of the APVs and other related viruses (Fig. 2), four of the APV sequences from black-headed caiques formed a cluster and two of the APV sequences from budgerigars formed a cluster. Adding with the other 48 partial APV genome sequences, more detailed analysis did not indicate host bird species-specific nucleotide sequences and amino acids (data not shown).

3.4. Analysis of the deduced amino acid substitution related with virus propagation in CEF culture

To investigate which amino acids in viral protein would be related with virus propagation in CEF culture, the whole genome sequences analysis of APV1 and APV4 was performed. According to the viral adaptation on BEF culture to CEF culture, viral genomic DNA was extracted from three different samples; therefore, its sequence was determined and compared. As the first sample, the liver sample of Bird 1 or Bird 4 was used. Second sample was the third passage of BEF culture inoculated with liver samples of Bird 1 or Bird 4, respectively. Third was the third passage of CEF culture adapted with each strain from BEF culture. As the results of comparison with three whole genome sequences each other, no deduced amino acid substitution in all viral proteins of both APV1 and APV4 was observed between the sequence from tissue sample and BEF culture. However, APV1 and APV4 adapted to CEF culture had single amino acid substitutions at position 221 (glycine to alanine in APV1 and valine in APV4, respectively) in viral structural protein VP2. No other predicted amino acid substitution was observed in all viral protein and no nucleotide change was detected in non-coding control regions in both strains.

3.5. Effect of deletion in VP4 on maturation of VP4 mRNA

To investigate the effects of the deletions detected in VP4 coding region of APV1 and APV2 on the splicing of VP4 mRNA, the sequence analysis of the matured VP4 mRNAs of APV1 and APV4 was performed. As the result of RT-PCR to amplify the region containing the deletion and first splicing positions, 197- or 206-bp products were detected in CEF culture inoculated with APV1 and APV4, respectively (Fig. 3). The results of sequence analysis of each PCR product revealed that 76 nt (position 33–108) or 77 nt (position 42–118) intron had been removed from pre-mRNA, respectively (data not shown). Thus, the splicing in

Table 3
Point mutations in seven strains of APVs compared with BFDV1.

Nucleotide number	Region	BFDV1	Nucleotide exchange compared with BFDV1 (amino acid substitution compared with predicted amino acid sequence of BFDV1)						
			APV1	APV2	APV3	APV4	APV5	APV6	APV7
34	Non-coding region	A	T	T	T	T	T	T	T
123	Non-coding region	C							T
343	VP4 (intron)	C				T	T		
371	VP4 (intron)	C	G	G	G	G	G	G	G
372	VP4 (intron)	G	C	C	C	C	C	C	C
460	VP4	G						A (G32R)	
670	VP4	T				C (F81L)	C (F81L)		
724	VP4	G				A (–)	A (–)		
742	VP4	T	C (–)	C (–)		C (–)	C (–)		
998	VP2	A			G (I8V)			G (I8V)	
1133	VP2	G		A (E53K)					
1137	VP2	C						A (T54K)	
1158	VP2	A		C (N61T)					
1288	VP2	C				A (–)	A (–)		
1459	VP2/VP3	T	A (–)	A (–)					
1474	VP2/VP3	C			T (–)			T (–)	
1540	VP2/VP3	G							A (–)
1592	VP2/VP3	A					C (T206P)		
1594	VP2/VP3	A					C (T206P)		
1638	VP2/VP3	T	G (V221G)	G (V221G)	G (V221G)	G (V221G)	G (V221G)	G (V221G)	G (V221G)
1670	VP2/VP3	C			G (Q232E)			G (Q232E)	
1677	VP2/VP3	G	A (R234H)	A (R234H)		A (R234H)	A (R234H)		
1694	VP2/VP3	T				A (S240T)	A (S240T)		
1749	VP2/VP3	C							T (P258L)
1765	VP2/VP3	C							T (–)
1775	VP2/VP3	G					C (E267Q)		
1792	VP2/VP3	A					G (–)		
1812	VP2/VP3	A					T (H279L)		
1878	VP2/VP3	A					T (Y301F)		
2415	VP1	C			G (R173E)				
2416	VP1	G			A (R173E)				
2463	VP1	G		A (–)					
2474	VP1	T							C (–)
2476	VP1	T					C (L193P)		
2478	VP1	T					A (Y194N)		
2512	VP1	A	G (K205R)	G (K205R)					
2558	VP1	G							A (–)
2663	VP1	A							C (–)
2745	VP1	G							A (–)
2881	VP1	T		G (–)					
2906	VP1	C							T (–)
2945	Non-coding region	C							A
3063	T-antigen	T			G (N575T)			G (N575T)	G (N575T)
3155	T-antigen	C							T (–)
3224	T-antigen								
3506	T-antigen	A	G (–)	G (–)		G (–)	G (–)		
3565	T-antigen	C					A (–)		
3579	T-antigen	C					A (–)		
3641	T-antigen	C			T (–)			T (–)	
3893	T-antigen	G							C (–)
3932	T-antigen	C						T (–)	
4125	T-antigen	A	G (L121P)	G (L121P)		G (L121P)	G (L121P)		
4241	T-antigen	C	A (–)	A (–)		A (–)	A (–)		
4292	T-antigen	A							G (–)
4433	T-antigen	A	T (–)	T (–)	T (–)	T (–)	T (–)	T (–)	T (–)
4502	T-antigen	A				G (–)	G (–)		C (–)
4504	T-antigen	G	A (–)	A (–)	A (–)	A (–)	A (–)	A (–)	A (–)
4649	t-antigen	C			T (–)				
4769	T/t-antigen	G							T (–)
4901	T/t-antigen	A			G (–)				
4949	T/t-antigen	A	C (C12G)	C (C12G)	C (C12G)	C (C12G)	C (C12G)	C (C12G)	C (C12G)
4972	T/t-antigen	A							G (–)
4976	T/t-antigen	A				C (–)	C (–)		

Minuses indicate the silent mutation positions. Blanks indicate identical nucleotide.

Table 4
Numbers of nucleotide and amino acid substitutions in this study compared with the sequence of BFDV1.

Strain	No. nucleotide substitutions	Predicted no. amino acid substitutions				
		VP1	VP2	VP3	VP4	Large T-antigen
APV1	15 (0.4)	1 (0.3)	2 (0.6)	2 (0.9)		2 (0.5)
APV2	19 (0.4)	1 (0.3)	4 (1.2)	2 (0.9)		2 (0.5)
APV3	17 (0.4)	2 (0.6)	3 (0.9)	2 (0.9)		2 (0.5)
APV4	20 (0.5)		3 (0.9)	3 (1.3)	1 (0.6)	2 (0.5)
APV5	30 (0.7)	2 (0.6)	7 (2.1)	7 (3.0)	1 (0.6)	2 (0.5)
APV6	16 (0.4)		4 (1.2)	2 (0.9)	1 (0.6)	2 (0.5)
APV7	25 (0.6)		2 (0.6)	2 (0.9)		2 (0.5)

Numbers in parentheses indicate percentages. Blank cells indicate no predicted amino acid substitution in the viral protein compared with BFDV1 sequence, but excluding deletions.

the VP4 mRNA of APV1 was not influenced by the deletions, suggesting that the matured VP4 mRNA of APV1 would consist of 522 bases, while that of APV4 consisted of 531 bases. These results indicate that 3 amino acid deletions (alanine–glycine–threonine) would be present in VP4 of APV1 and APV2, respectively.

3.6. Effect of deletion in VP4 on viral infectivity

To analyze the viral propagation of both viruses having deletion or no deletion in VP4 on CEF culture, infectivity in the supernatants and cells infected with isolate having three amino acids deletion isolate (APV1) and no deletion isolate (APV4) was titrated (Fig. 4). The infectivities of APV1 in both the supernatant and cells were generally very similar to those of APV4. Significant differences were found only at 24 h.p.i. in the supernatant and at 36 h.p.i. in the cells, at which times the titers were 10-fold higher for APV1.

4. Discussion

In the present study, the genetic diversity of APV isolates was investigated by the whole genome sequencing analysis. The multiple alignment analysis of the whole genome sequence of 7 APV isolates in Japan between 2003 and 2006 and GFM-1 strain demonstrated a small amount of variation. Excluding deletions, scattered 63 variable nucleotide positions were found in the whole genome. This corresponds to 99.4–99.7% nucleotide homology between each sequence in this study and the sequence of the BFDV strain. The present results indicate a high level of genome conservation as reported by other researchers.

In the present study, we showed that substitution of glycine for alanine or valine at position 221 was essential

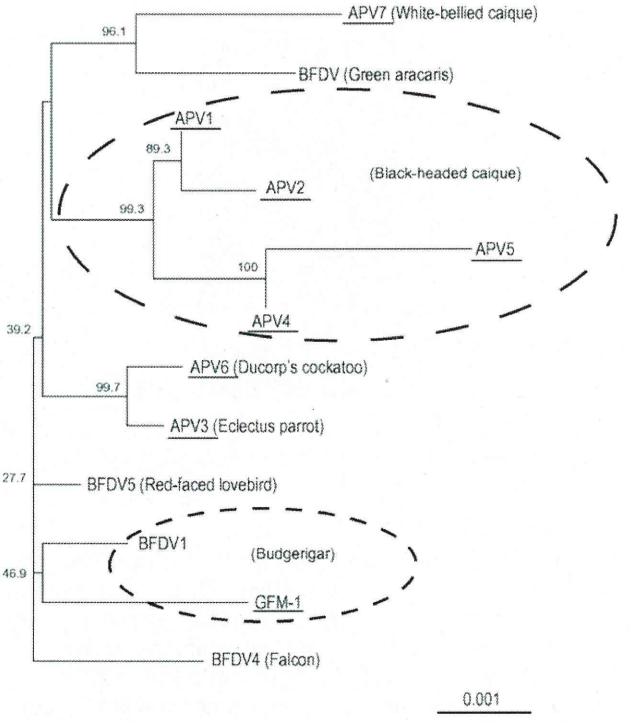

Fig. 2. Bootstrapped phylogenetic tree obtained using the neighbor-joining method based on the nucleotide sequences of the whole genome sequence of APV. APV strains generated in this study are underlined and other sequences were obtained from the GenBank database. The numbers at the nodes indicate the bootstrap values. Bird species from which the indicated strains were obtained are shown in parentheses.

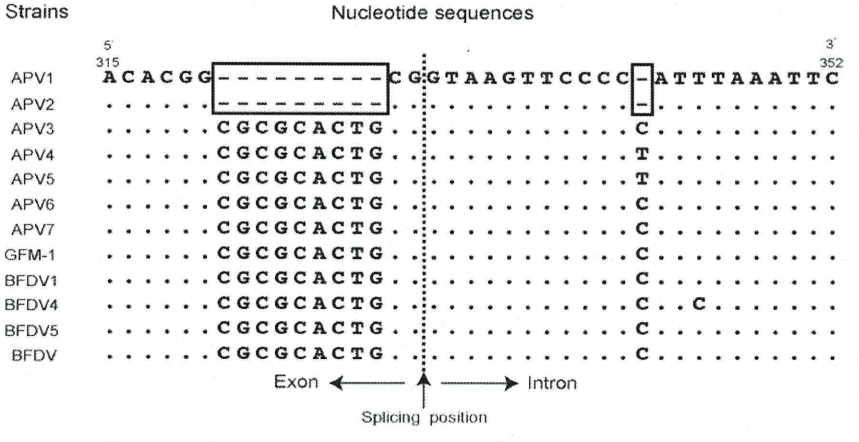

Fig. 1. Comparison of the partial nucleotide sequence of VP4 region of 12 APV genomes including 4 sequences derived from the database. Deletions in APV1 and APV2 are boxed. The splicing position is indicated by the vertical arrow and dotted line. Exon and intron regions are indicated by horizontal arrows. Dots indicate identical nucleotides.

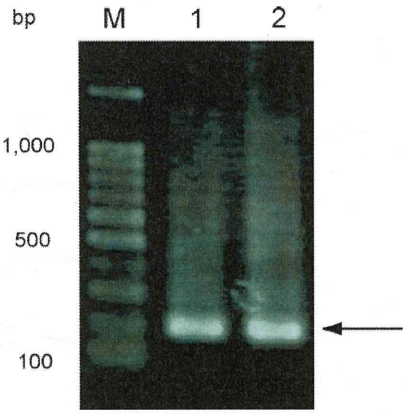

Fig. 3. RT-PCR analysis of the matured APV VP4 mRNA. The positions of the specific products are indicated by arrow (approximate 200 bp). Lane 1, APV1; Lane, 2, APV4; M, 100 bp DNA Ladder (ToYoBo, Osaka, Japan).

for APV isolates to propagate on CEF culture. Similarly, Bozeman et al. (1981) reported that APV isolated could be easily adapted to grow in CEF culture after several passages in BEF culture. Stoll et al. (1994) demonstrated based on hybrid genomes that one amino acid at position 221 in the common region of the VP2/3 determined the efficiency of viral replication in CEF culture (Stoll et al., 1994). On the other hand, Phalen et al. (1999) reported that some cell culture viruses having a gylcine at 221 could grow in CEF culture, therefore the glycine inhibits replication in CEF culture from certain strains of chicken. As the explanation for this discrepancy, the results of Phalen et al. were based on the sequences amplified from tissue culture prepared with naturally APV-infected birds not from CEF culture after adaptation. The results in this study showed that the mutation did not occur during passage in BEF culture, whose cells are derived from Psittaciformes, even after three passages. Thus, it was hypothesized that mutant APV, which could grow in CEF culture, should be included in the population and that the level of the mutants might be too low to be detected. Once the APV population was inoculated in CEF culture, a kind of mutant, which might have advantage in grow in CEF culture, would be expected to be the major group to be detected. A possible explanation for the growth of APV7 in CEF culture without inoculation in BEF culture is that a virus having this mutation naturally exists in the population of the liver sample. APVs exhibit a broad host range compared to the highly specific host range of mammalian polyomaviruses (Perez-Losada et al., 2006). Further studies are needed to confirm the interaction between VP2/VP3 and host factors.

The amino acid deletions in VP4 in the present study had little effect on viral propagation (Fig. 4). Deletion mutants of VP4 were infectious but had slower replication kinetics and lower end-point titers than the wild-type virus (Johne et al., 2007). Although VP4 has multiple potential phosphorylation sites (Liu and Hobom, 2000), the three amino acids deleted in this study were not located at a phosphorylation site. VP4 has a typical leucine zipper motif, and is proposed to have a multimerization domain (Johne and Muller, 2001). Because these domains are in the central part of VP4, their function should not be affected by the deletion. Further studies are needed to clarify the relation between these deletions and the function of VP4 including induction of apoptosis, which is thought to be another property of this protein (Johne et al., 2000).

Avian species serve humans in several ways, such as livestock animals (e.g. chickens and turkeys), companion animals (e.g. budgerigars and lovebirds), and labor-birds (e.g. pigeons and cormorants). In addition, avian species are key models for studies of vertebrate development and gene function (Stern, 2005). However, to date, the SV40 promotor is commonly used for transient expression of transgenes in not only mammalian cells but also avian cells. The promotor region of APV has been reported to be smaller than the promotor regions in SV40 and other polyomaviruses: the APV genome contains a 45-bp tandem repeated sequence as the transcriptional control region, in contrast to the 72-bp segments of SV40. In addition, the APV genomic sequence has no potential signal for SP-1 binding adjacent to the putative promotor element, which is observed in the SV40 genome (Luo et al., 1994; Rott et al., 1988). Thus, the development of transient expression technologies adapted for use in avian systems will be important. Three regions in the APV isolates examined in this study (the putative replication origin, the transcriptional control region, and the polyadenylation sites) were

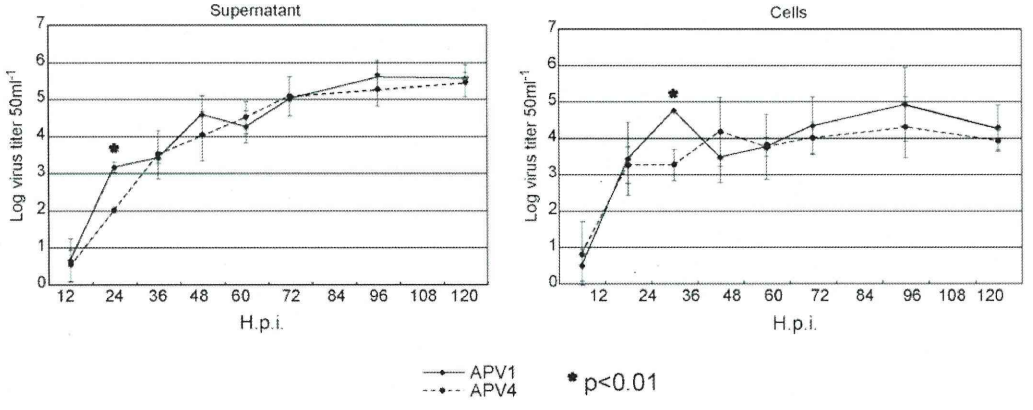

Fig. 4. Titration of infectivity of APV1 and APV4 in CEF cell culture. Titers of virus released into the supernatant are shown in the left diagram and titers of cell-associated virus released from cells after three cycles of freezing and thawing are shown on the right. H.p.i., hours post-infection.